

## Dalton Transactions

# Synthesis and Characterization of Borohydride Rare-Earth Complexes Supported by 2-PyridinemethanAmido Ligands and their Application towards Ring-Opening Polymerization of Cyclic Esters

Journal:	Dalton Transactions
Manuscript ID	DT-ART-09-2024-002522.R1
Article Type:	Paper
Date Submitted by the Author:	11-Oct-2024
Complete List of Authors:	Beauvois, Maxime; Université de Lille, Unité de Catalyse et Chimie du Solide Capet, Frédéric; Université Lille 1 Sciences et Technologies, UMR 8181 CNRS, Unité de Catalyse et Chimie du Solide 'UCCS', Ziller, Joseph; University of California, Irvine, Department of Chemistry Evans, William; University of California- Irvine, Department of Chemistry Champouret, Yohan; Université de Lille, Unité de Catalyse et Chimie du Solide Visseaux, Marc; Université de Lille, Unité de Catalyse et Chimie du Solide, UMR CNRS 8181; Centrale Lille ENSCL,

SCHOLARONE™ Manuscripts

## Synthesis and Characterization of Borohydride Rare-Earth Complexes Supported by 2-PyridinemethanAmido Ligands and their Application towards Ring-Opening Polymerization of Cyclic Esters

Maxime Beauvois,<sup>a</sup> Frédéric Capet,<sup>a</sup> Joseph W. Ziller,<sup>b</sup> William J. Evans,<sup>b</sup> Yohan Champouret,\*,<sup>a</sup> Marc Visseaux\*,<sup>a</sup>

<sup>a</sup> Univ. Lille, CNRS, Centrale Lille, Univ. Artois, UMR 8181, UCCS, Unité de Catalyse et Chimie du Solide, F-59000, Lille, France. E-mail : Yohan.champouret@univ-lille.fr, Marc.visseaux@univ-lille.fr.

#### Abstract.

The synthesis of 2-pyridinemethanamido borohydride complexes of yttrium and neodymium was achieved through the in situ deprotonation of the protio-ligand 2-pyridinemethanamine C₅H₃R₁N- $C(CH_3)R_2-NH(2,6-Pr_2C_6H_3)$ , noted as **PyAH** (with **PyAH**<sup>1</sup>:  $R_1 = R_2 = H$ ; **PyAH**<sup>2</sup>:  $R_1 = CH_3$ ,  $R_2 = H$ ; **PyAH**<sup>3</sup>:  $R_1 = R_2 = H$ ; **PyAH**<sup>3</sup>:  $R_2 = H$ ; **PyAH**<sup>3</sup>:  $R_3 = H$ ; **PyAH** =  $C(CH_3)=N-(2,6^{-1}Pr_2C_6H_3)$ ,  $R_2=CH_3$ ), in the presence of the trisborohydride  $RE(BH_4)_3(THF)_3$  (RE = Y, Nd) as a precursor and a base. The isolation of various molecular structures, nine of which were structurally characterized by X-ray diffraction analysis, was obtained and revealed to depend not only on i) the nature of the 2-pyridinemethanamido ligand and ii) the rare-earth element but also ii) the reaction conditions, notably the type of base used. These include seven mono-substituted species, eventually also comprising the cation issued from the base reagent, such as  $[(\mathbf{PyA^1})Y(\mathbf{BH_4})_3]_2[\mathbf{Mg}(\mathbf{THF})_6]$   $(\mathbf{1}_Y)$ ,  $[(PyA^1)Nd(BH_4)_3Mg(PyA^1)](THF)_4$   $(1_{Nd})$ ,  $(PyA^1)Nd(BH_4)_2(THF)_2$   $(1'_{Nd})$ ,  $[(PyA^1)Nd(THF)(BH_4)(\mu-BH_4)]_2$  $(1''_{Nd})$ ,  $[(PyA^2)Nd(BH_4)_3]_2[Mg(THF)_6](3_{Nd})$ ,  $(PyA^2)Nd(BH_4)_2(THF)_2(3'_{Nd})$  and  $(PyA^3)Nd(BH_4)_2(4_{Nd})$ , as well as two bis-substituted complexes  $(PyA^1)_2Y(BH_4)$   $(2_Y)$  and  $(PyA^1)_2Nd(BH_4)$   $(2_{Nd})$ . On the other hand, the unexpected amido/ene-amido derivative  $[(PyA(EA))Y(BH_4)_2][Li(THF)_4]$  (5<sub>Y</sub>) (PyA(EA): R<sub>1</sub> = C=CH<sub>2</sub>-N(2,6- $^{\prime}$ Pr<sub>2</sub>C<sub>6</sub>H<sub>3</sub>)-, R<sub>2</sub> = CH<sub>3</sub>), where the **PyAH**<sup>3</sup> protio-ligand underwent double deprotonation, was recovered from the reaction carried out with "BuLi in the yttrium series. In some cases, the synthesis led to the isolation borohydride 2-pyridinemethanamido-supported magnesium (PyA<sup>2</sup>)Mg(BH<sub>4</sub>)(THF) and (PyA<sup>3</sup>)Mg(BH<sub>4</sub>)(THF). In parallel, PyAH<sup>2</sup> pro-ligand could be structurally analyzed, and an unprecedented adduct of the type [KN(SiMe<sub>3</sub>)<sub>2</sub>.PyAH<sup>1</sup>]<sub>2</sub> was isolated and characterized by X-ray diffraction analysis. Preliminary investigations in Ring-Opening Polymerization of L-lactide and  $\varepsilon$ -caprolactone with some of the complexes synthesized are finally presented, demonstrating moderate to high catalytic activities.

#### 1. Introduction

Coordination chemistry is regularly seeking to diversify, with the ambition of producing complexes that can be used in ever-expanding fields of application, through the engineering of organic ligands that can be adapted to different metals. In particular, the design of ligands incorporating nitrogen atoms has been successfully applied to develop a large number of metal-based complexes for a wide range of applications. Among them, 2-pyridinemethanamino/amido ( $PyAH/PyA^-$ ) systems of the type  $C_5H_4N-C(R_2)-NH(R')/C_5H_4N-C(R_2)-N(R')$  (R=alkyl or H; R'=alkyl or aryl), and their related structures, are of great interest as ligands due to i) the ease of synthesis of the protonated amino counterpart PyAH, which is achieved by a simple condensation reaction of a suitable amine on the pyridyl-ketone precursor, followed by a reduction reaction of the imine group and ii) the possibility of modification

<sup>&</sup>lt;sup>b</sup> Department of Chemistry, University of California, Irvine, California 92697-2025, United States

on multiple sites, which allows a rich variation of coordination and/or electronic/steric properties on the resulting metal-based complex.

Since the isolation of a Zn complex with a PyA ligand by M. Westerhausen,2 various ligand modifications and their coordination chemistry with several metal-based systems have been explored. These include, among others, applications in polymerization reactions with Groups 4 and 10 metals<sup>3</sup> and Ring-Opening Polymerization (ROP) of lactide with iron<sup>4</sup> or Group 12 metals.<sup>5</sup> Rare-earth complexes, in particular non-Cp derivatives, <sup>6</sup> have also been extensively studied over the past three decades, focusing on complexes with nitrogen-based ligands (e.g.: amidinate, amidopyridinate, guadinidate,  $\beta$ -diketiminate...), which have been applied in homogeneous catalysis.<sup>7</sup> Several rare-earth complexes with 2-pyridinemethanamido derivatives have been synthesized since 2003, some of them used in polymerization catalysis. The Gordon group reported a lutetium complex with a tridentate amido-pyridine-imine ligand,8 while Anwander and colleagues expanded this finding to other rareearth metals, enabling the identification of key intermediates in ethylene polymerization. 9 Studies by Trifonov and Giambastiani on the substitution of imino groups by (hetero)aryl ones led to C-H bond activation.  $^{10,11}$  Zhou, Wang, and Luo prepared dianionic  $\alpha$ -iminopyridine rare-earth alkyl complexes for polymerization and coupling reactions. 12 The group of Cui demonstrated the ability of rare-earth metal bis(alkyl) complexes (Sc, Lu and Y) with a bidentate PyA ligand to polymerize both isoprene and ethylene monomers.<sup>13</sup> In addition, various monoanionic quinolinyl anilido rare-earth complexes, including Sc,14 Lu, Nd and Y derivatives, have been used for the (co)polymerization of 1,3-dienes and styrene but also for polar alkoxystyrene monomers. 15,16 Finally, rare-earth metal complexes bearing amido-trihydroquinoline ligands have also been described, demonstrating moderate catalytic activity for 1,4-stereoselective isoprene polymerization.<sup>17</sup>

In view of these literature data, it is clear that with the exception of the work by Cui cited above,<sup>13</sup> with a single crystal structure of a Nd complex ligated to **PyA**, the rare-earth complexes prepared with this type of ligand are all based on a metal belonging to the late series. It is therefore interesting to propose a comparison with other complexes based on a lanthanide in the early series with a larger ionic radius. In that context, we focus our attention in the present study on three different monoanionic 2-pyridinemethanamido ligands **PyA¹**, **PyA²**, **PyA³** that are issued from the corresponding 2-pyridinemethanimines **PyAH** (Chart 1).

Chart 1 The 2-pyridinemethanamine PyAH¹-PyAH³ protio-ligands studied in this work

The impact of the substituent of the PyA ligands in the 6-position of the pyridine ring [H for  $PyA^1$ , Me for  $PyA^2$  and  $C(Me)=N-(2,6-Pr_2C_6H_3)$  for  $PyA^3$ ] towards the coordination chemistry with Y and Nd, two typical representatives of the "late" and of the "early" sub-group, will be presented herein. In the unprecedented complexes described herein, where the rare-earth metal is coordinated by both PyA and trisborohydride ligands, the presence of trisborohydride on the rare-earth metal also offers the advantages of exceptional reactivity, the ability to isolate well-defined species, and significant potential for application in the ROP of cyclic esters. 6f

The inorganic complexes isolated in this work are depicted in Chart 2.

**Chart 2** The new 2-pyridinemethanamido and related complexes synthesized in this work, which have been characterized by DRX and/or elemental analyses.

# 2. Syntheses of 2-pyridinemethanamine protio-ligands and attempts to isolate the related anionic 2-pyridinemethanamido compounds

Although the synthesis of **PyAH**<sup>1</sup> and **PyAH**<sup>3</sup> has been known for many years (Scheme 1.a and 1.c, respectively), <sup>18</sup> the ligand **PyAH**<sup>2</sup> was recently developed in our research group starting from the 6-bromo-2-picoline according to Scheme 1.b.<sup>4</sup> The first step in the synthesis of **PyAH**<sup>2</sup> was the preparation of 1-(6-methylpyridin-2-yl)ethan-1-one, from the lithiation of commercially available 6-bromo-2-picoline with <sup>n</sup>BuLi, followed by addition of *N,N*-dimethylacetamide. Subsequently, the condensation reaction of 2,6-diisopropylaniline with the corresponding ketones was undertaken, which allowed to obtain the three different imine precursors as previously described. While **PyAH**<sup>1</sup> and **PyAH**<sup>2</sup> were issued in the last step of their synthesis from the reduction of N-(2,6-diisopropylphenyl)-1-(pyridin-2-yl)ethan-1-imine and N-(2,6-diisopropylphenyl)-1-(6-methylpyridin-2-yl)ethan-1-imine with an excess of NaBH<sub>4</sub>, respectively, **PyAH**<sup>3</sup> was obtained by the mono-reduction and alkylation of 2,6-bis[1-(2,6-diisopropylphenylimino)ethyl]pyridine using trimethyl aluminum (AlMe<sub>3</sub>), followed by hydrolysis. <sup>18b</sup>

Scheme 1 Synthesis of protio-ligand PyAH1 (a), PyAH2 (b) and PyAH3 (c)

Unprecedently, we obtained single crystals of  $PyAH^2$  suitable for X-ray diffraction (XRD) analysis from a slow evaporation of a  $CH_2Cl_2$  solution containing the ligand. This compound crystallized in  $Pca2_1$  space group, a view of  $PyAH^2$  is shown in Fig. 1, selected bond distances and angles are listed in Table 1. The molecular structure of  $PyAH^2$  shows the two enantiomers (R) and (S) in the unit cell with a conformation similar to that of  $PyAH^1.180$  The C-N(amine) bond distance [C13-N1 = 1.478(3) Å] is comparable to that of  $PyAH^1$  and is in the typical range for a  $C(sp^3)-N$  amine bond length. Both nitrogen atoms are in a *quasi-cis* position relative to each other, as a weak non-bonding H1-N2<sub>Pyr</sub> interaction<sup>19</sup> is present with a distance of 2.588(2) Å, as previously noticed for  $PyAH^1$  (position of the hydrogen calculated by the X-ray software). Further information on the structural description is given in the SI section (Table S1).

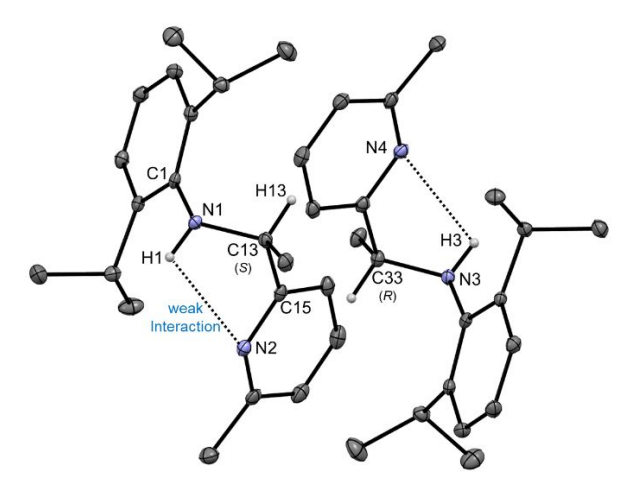


**Fig. 1** Molecular structure of **PyAH**<sup>2</sup> (*R* and *S*), hydrogen atoms have been omitted for clarity apart for H1 and H3. Thermal ellipsoids are drawn at the 30% probability level.

To our knowledge, the preparation of 2-pyridinemethanamido supported rare-earth derivatives described in the literature has been typically achieved by *in situ* deprotonation of the protonated ligand with tris-alkyl rare-earth precursors.<sup>8,13</sup> The synthesis of borohydride rare-earth complexes in

this 2-pyridinemethanamido series, which may require salt metathesis from pre-formed anionic ligands, does not seem to have been investigated to date. The deprotonation of PyAH1 with "BuLi or KH, as reported for guanidinate<sup>20</sup> or cyclopentadienyl<sup>21</sup> ligands, proved unsuccessful in isolating MPyA<sup>1</sup> (M = Li, K) with satisfactory yield/purity for subsequent synthetic steps. In contrast, upon addition of KN(SiMe<sub>3</sub>)<sub>2</sub> to a solution of **PyAH**<sup>1</sup>, a color change was observed. However, monitoring the reaction by <sup>1</sup>H NMR in THF-d<sub>8</sub> revealed no significant difference compared to the protonated ligand alone, aside from an additional resonance at  $\delta = -0.20$  ppm, corresponding to KN(SiMe<sub>3</sub>)<sub>2</sub> (see experimental section, Fig. S1). After heating the solution at 50 °C for one week and monitoring the reaction by ¹H NMR, no change of the PyAH1 resonances was observed in the 1H spectrum, suggesting that if an adduct is formed, it rapidly dissociated in solution. Interestingly, crystals suitable for XRD determination were obtained at -35 °C from a concentrated solution of this mixture in pentane. Elemental analysis of these crystals was consistent with the molecular formula KN(SiMe<sub>3</sub>)<sub>2</sub>.**PyAH**<sup>1</sup>, indicating that the adduct is stable in the solid state. The molecular structure of this isolated compound, of P-1 space group symmetry, is depicted in Fig. 2 and displays a dimeric species with two silyl amido bridging groups [N(SiMe<sub>3</sub>)<sub>2</sub>] linked to two potassium atoms, each of which is additionally bound to one protonated ligand PyAH1. This arrangement leads to a structure of the form [KN(SiMe<sub>3</sub>)<sub>2</sub>.PyAH1]<sub>2</sub> (hereafter noted KN.PyAH<sup>1</sup>). Selected bond distances and angles are listed in Table 1.

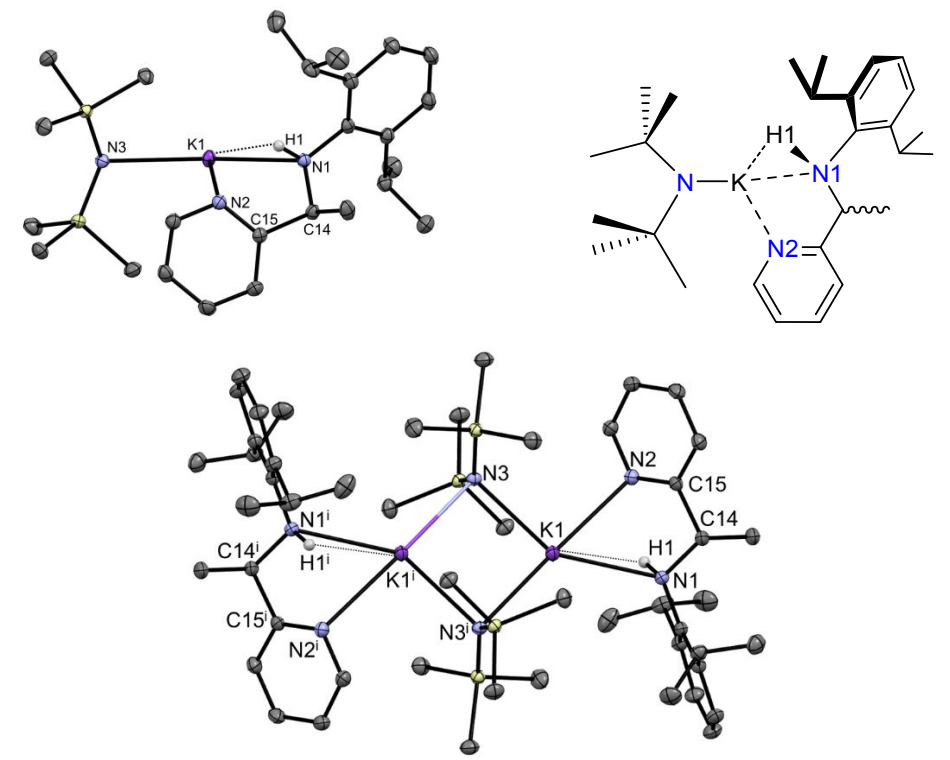


**Fig. 2** Partial molecular structure of  $[KN(SiMe_3)_2.PyAH^1]_2$  (up, ORTEP and Chemdraw drawing) and total view (down) where hydrogen atoms have been omitted for more clarity apart for H1 and H1<sup>i</sup>. Thermal ellipsoids are drawn at the 30% probability level.

The structural differences between the free ligand  $PyAH^1$  and its potassium amide adduct  $KN.PyAH^1$  result from a change in the distance of interaction between H1 and N2 atoms, which becomes shorter in the latter [H1-N2 = 2.186(11) Å vs. H1-N2 = 2.651 Å<sup>18a</sup> in  $PyAH^1$ ]. Furthermore, the H1-N1 [0.878(16) Å] and the C14-N1(amine) [1.479(1) Å] bond distances in the adduct  $KN.PyAH^1$  remain relatively close in value compared to that described for  $PyAH^1$  [H1-N1 = 0.903 Å and C13-N1 = 1.462 Å]. The potassium center is at nearly equal distance from the nitrogen atoms of the chelating  $PyAH^1$  ligand

[K1-N1(amine) = 2.9873(9) Å and K1-N2(Pyr) = 3.0474(7) Å]. The bridging nitrogen atoms N3 of the silyl amide group is linked to one potassium atom by a X-type bond [K1-N3 = 2.7513(8) Å], which is similar to the K-N bond distance in KN(SiMe<sub>3</sub>)<sub>2</sub> (K-N = 2.77 Å),<sup>22</sup> while it is connected to the other K atom as a L-type bond, which is found to be slightly longer [K1<sup>i</sup>-N3 = 2.8447(7) Å] than the K-N distance in KN(SiMe<sub>3</sub>)<sub>2</sub>. More details on the structural description are provided in the SI section (Table S1).

	PyAH <sup>1</sup>	PyAH <sup>2</sup>	KN.PyAH <sup>1</sup>
N1-H1 (Å)	0.903	0.880(2)	0.878(16)
N2 <sup></sup> H1 (Å)	2.651	2.588(2)	2.186(11)
C13-N1 (Å)	1.462(2)	1.478(3)	1.479(1) <b>(C14-N1)</b>
K1-N1 (Å)	na	na	2.9873(9)
K1-N2 (Å)	na	na	3.0474(7)
K1-N3 (Å)	na	na	2.7513(8)
N2-C15-C13-N1 (°)	-66.4(2)	-54.6(3)	-20.49(10) <b>(N2-C15-C14-N1</b> )
Pyr vs. Aryl plane (°)	60.58	67.04(9)	45.62(4)

#### 3. Synthesis of rare-earths complexes

#### 3.1. (PyA¹)-supported yttrium complexes

With the aim to isolate a mono-substituted  $PyA^1$  yttrium compound, the synthesis was performed in toluene in the presence of BEM/ $PyAH^1$ /Y(BH<sub>4</sub>)<sub>3</sub>(THF)<sub>3</sub> = 0.5/1/1 (Scheme 2) using a strategy described as the "borohydride/alkyl" (B/A) route in previous works carried out by some of us.<sup>23</sup> After work-up, a powdery material was isolated in good yield, which elemental analysis (see experimental section) was in accordance with a heterobimetallic trinuclear "ate" yttrium-magnesium complex ( $\mathbf{1}_Y$ ) of the form  $[(PyA^1)Y(BH_4)_3]_2[Mg(THF)_6]$  in the solid state, as observed in the case of mono-cyclopentadienyl lanthanide derivatives.<sup>23a-c</sup>

Scheme 2 Synthesis of the complex  $[(PyA^1)Y(BH_4)_3]_2[Mg(THF)_6]$ ,  $\mathbf{1}_Y$ .

The  $^1$ H NMR spectrum of  $\mathbf{1}_{Y}$  in  $C_6D_6$  revealed a significant shift compared to the free protio-ligand signals and the yttrium-(BH<sub>4</sub>) initial resonance, with the expected number of signals that agree with the formation of  $\mathbf{1}_{Y}$  (Fig. S2a, and  $^{13}$ C NMR spectrum in Fig. S3, SI section<sup>†</sup>). Crystallization from a cold, concentrated THF solution of  $\mathbf{1}_{Y}$  with a pentane layer afforded a high yield of crystals suitable for XRD (see Section 4, crystallography part).

In an attempt to generate a bis-substituted  $PyA^1$  yttrium complex, the reaction of BEM/ $PyAH^1$ /Y(BH<sub>4</sub>)<sub>3</sub>(THF)<sub>3</sub> = 1/2/1 was carried out at the NMR scale, but unexpectedly, the resulting  $^1H$  NMR spectrum revealed that the mono-substituted derivative was still the major product (Fig. S2b, SI section†). One can thus conclude that the use of the BEM reagent seems inappropriate to cleanly afford a bis-( $PyA^1$ )-Y derivative.

In order to check if a mono-substituted yttrium complex that was Mg-free was accessible, a synthesis was carried out in toluene using MeLi [MeLi/**PyAH¹**/Y(BH₄)₃(THF)₃ = 1/1/1] instead of BEM (Scheme 3). After work-up, a small crop of yellow X-ray quality crystals could be isolated after allowing the toluene solution to stand at low temperature with a layer of pentane. Surprisingly, XRD analysis revealed that this compound was the bis-substituted derivative (**PyA¹**)₂Y(BH₄) (**2**<sub>Y</sub>) (see Section 4, crystallography part and ¹H and ¹³C NMR spectra in Figs. S4a-b, SI section†). It is likely that the absence of any Mg counterpart, in that case, did not allow the isolation of a stable mono-(**PyA¹**)-substituted complex in the solid state, which underwent ligands redistribution leading to **2**<sub>Y</sub>.²⁴ Unfortunately, no satisfactory elemental analysis could be obtained for **2**<sub>Y</sub>.

**Scheme 3** Proposed formation of  $(PyA^1)_2Y(BH_4)_2$ ,  $2_Y$  from the mono- $(PyA^1)$ -substituted yttrium derivative.

Regardless of the  $PyA^1/Y(BH_4)_3(THF)_3$  ratio, we propose that the mono- $(PyA^1)$ -Y derivative is stable only when combined with a Mg counterpart originating from the BEM reagent, leading to the formation of a heterobimetallic "ate" compound. When an organolithium reagent is employed, the bis- $(PyA^1)$ -Y complex can be isolated, whereas this complex seems inaccessible when using BEM.

#### 3.2. (PyA1)-supported neodymium complexes

In a similar way to yttrium, we firstly performed the reaction in THF with BEM/ $PyAH^1$ /Nd(BH<sub>4</sub>)<sub>3</sub>(THF)<sub>3</sub> = 0.5/1/1 ratio. After work-up, which allowed elimination of presumably Mg(BH<sub>4</sub>)<sub>2</sub> salts (see experimental part), a green crude solid was isolated in good yield (*ca.* 78%). <sup>1</sup>H NMR analysis of this compound in C<sub>6</sub>D<sub>6</sub> is depicted in Fig. S5 (SI section). Elemental analysis of this compound, here designed as complex  $\mathbf{1'}_{Nd}$  (Scheme 4, path a), was in accordance with the molecular formula ( $PyA^1$ )Nd(BH<sub>4</sub>)<sub>2</sub>(THF)<sub>2</sub> (see experimental section).

Attempt synthesis of the bis-(PyA1)-substituted Nd derivative was then undertaken with BEM/**PyAH** $^{1}$ /Nd(BH $_{4}$ ) $_{3}$ (THF) $_{3}$  = 1/2/1 ratio (Scheme 4, path b). The  $^{1}$ H NMR paramagnetic spectrum in  $C_6D_6$  of the isolated solid (Fig. S6, SI section<sup>†</sup>) was identical to  $\mathbf{1'}_{Nd}$  (Fig. S5, SI section<sup>†</sup>), revealing that this spectrum was again the signature of a mono (PyA¹)-substituted complex. Yet, elemental analysis of the isolated material was this time in accordance with a compound comprising two PyAH1 ligands with Nd and Mg, such as (PyA¹)<sub>2</sub>Nd(BH<sub>4</sub>).Mg(BH<sub>4</sub>)<sub>2</sub>(THF)<sub>4</sub>, as already described in the cyclopentadienyl series, where Mg(BH<sub>4</sub>)<sub>2</sub> remains associated to Nd under a heterobimetallic compound.<sup>23d</sup> Nevertheless, а molecular formula such as  $[(\mathbf{PyA^1}) \mathrm{Nd}(\mathrm{BH_4})_2.(\mathrm{BH_4}) \mathrm{Mg}(\mathbf{PyA^1})](\mathrm{THF})_4$  $[(\mathbf{PyA^1}) \text{Nd}(\mathbf{BH_4})_3] [Mg(\mathbf{PyA^1})] (THF)_4]$ , noted as  $[(\mathbf{PyA^1}) \text{Nd}(\mathbf{BH_4})_3 Mg(\mathbf{PyA^1})] (THF)_4$  ( $(\mathbf{1}_{Nd})$ , Scheme 4, path b) is more likely to be formed, as the <sup>1</sup>H NMR spectrum supports the presence of a mono (PyA¹)substituted Nd complex.

Scheme 4 Isolation of a) the mono-substituted (PyA¹)Nd(BH<sub>4</sub>)<sub>2</sub>(THF)<sub>2</sub> ( $\mathbf{1'}_{Nd}$ ) and b) dimeric complex [(PyA¹)Nd(THF)(BH<sub>4</sub>)( $\mu$ -BH<sub>4</sub>)]<sub>2</sub> ( $\mathbf{1''}_{Nd}$ ), issued from  $\mathbf{1}_{Nd}$ .

Thankfully, a crop of X-ray quality crystals (ca. 50 mg) could be obtained upon standing the solution in toluene/pentane at low temperature (-40 °C). After XRD analysis, this crystallized compound revealed to be a dimeric mono-substituted complex [( $PyA^1$ )Nd(THF)(BH<sub>4</sub>)( $\mu$ -BH<sub>4</sub>)]<sub>2</sub>,  $1''_{Nd}$  (see Section 4, crystallography part), lacking Mg moiety, probably resulting from a ligand exchange process occurring during crystallization. The  $^1$ H NMR analysis of the crystals of  $1''_{Nd}$ , with paramagnetic signals identical to  $1_{Nd}$  and  $1'_{Nd}$ , confirmed the formation of a mono-( $PyA^1$ )-Nd complex in the bulk solution synthesis, ruling out the access to a bis-( $PyA^1$ )-substituted compound with BEM, as observed for yttrium. Unfortunately, several attempts to obtain a suitable elemental analysis for complex  $1''_{Nd}$  have failed. Ultimately, a conclusive  $^1$ H NMR scale experiment provided convincing evidence regarding the formation of a mono-( $PyA^1$ )-substituted Nd borohydride complex. This was achieved through the reaction of ( $C_3$ H<sub>5</sub>)Nd(BH<sub>4</sub>)<sub>2</sub>(THF)<sub>3</sub>, a mixed allylborohydride Nd complex that is known to react with protic molecules,  $^{25}$  with 1 equiv. of  $PyAH^1$  (Scheme 5). The resulting  $^1$ H NMR spectrum in  $C_6D_6$  (Fig. S6, SI section†) was found to be identical to those described above for the three mono-substituted complexes  $1_{Nd}$ ,  $1'_{Nd}$  and  $1''_{Nd}$  in the same NMR solvent, despite a difference in coordination in the solid state of these complexes.

$$(BH_4)$$
 propene 
$$C_7D_8$$
 
$$THF$$
 + PyAH<sup>1</sup> 
$$C_7D_8$$
 smooth heating 
$$(BH_4)$$
 . x THF

Scheme 5 Reaction of (C<sub>3</sub>H<sub>5</sub>)Nd(BH<sub>4</sub>)<sub>2</sub>(THF)<sub>3</sub> with 1 equiv. of PyAH<sup>1</sup>

Intrigued by the isolation of such a mono-( $PyA^1$ )-substituted Nd complex even in the presence of 2 equiv. of  $PyA^1$  ligand with a large Nd center in the reaction mixture, we sought to reconsider the reaction of Nd( $BH_4$ )<sub>3</sub>(THF)<sub>3</sub> precursor in the presence of 2 equiv. of  $PyAH^1$  with an organolithium base instead of BEM.

The reaction of Nd(BH<sub>4</sub>)<sub>3</sub>(THF)<sub>3</sub> with 2 equiv. of **PyAH**<sup>1</sup> and MeLi was then performed in toluene (Scheme 6). To our delight, this synthesis afforded, after work-up, green single crystals suitable for XRD, although in poor yield (19%), which allowed us to acquire the molecular structure of the isolated complex as the bis-substituted (**PyA**<sup>1</sup>)<sub>2</sub>Nd(BH<sub>4</sub>),  $\mathbf{2}_{Nd}$  (see Section 4, crystallography part). The <sup>1</sup>H NMR spectrum in C<sub>6</sub>D<sub>6</sub> of these crystals revealed a different set of paramagnetic signals (Fig. S7, SI section<sup>†</sup>) compared to the <sup>1</sup>H NMR spectrum of  $\mathbf{1}_{Nd}$  (and analogs  $\mathbf{1}'_{Nd}$ ,  $\mathbf{1}''_{Nd}$ ), consistent with the formation of a new (**PyA**<sup>1</sup>)-supported Nd complex.

Scheme 6 Synthesis of complex 2<sub>Nd</sub>

To summarize, it appears that the syntheses and isolation of complexes comprising a 2-pyridinemethanimido ligand (PyA¹) are highly alkylating reagent dependent. Indeed, when BEM was employed as co-reagent, mono-(PyA¹)-substituted Y or Nd complexes, potentially including a Mg moiety, can be isolated, while the bis-(PyA¹)-substituted derivatives seem inaccessible. In contrast, with organolithium bases, bis-(PyA¹)-substituted Y or Nd complexes can be formed that furthermore do not contain any lithium counterpart in their molecular structure. These features seem to apply to both small Y and large Nd.

#### 3.3. (PyA<sup>2</sup>)-supported complexes

The attempted synthesis of a mono-(**PyA**<sup>2</sup>)-substituted complex in the yttrium series failed to afford a clean product, either in the presence of BEM or alkyl lithium bases. Crystallization attempts of a bulk toluene mixture of Y(BH<sub>4</sub>)<sub>3</sub>(THF)<sub>3</sub>/**PyAH**<sup>2</sup> in the presence of 0.5 equiv BEM resulted in the isolation of a small crop of yellow single-crystals suitable for X-ray diffraction studies. Unexpectedly, the X-ray structure determination established the formula (**PyA**<sup>2</sup>)Mg(BH<sub>4</sub>)(THF) for that complex, lacking yttrium (see Fig. S14, SI section<sup>†</sup>). This magnesium derivative could result from ligand exchange in solution during crystallization just after formation of the desired (**PyA**<sup>2</sup>)-supported yttrium product (Scheme 7). This kind of exchange between magnesium and rare-earth species has already been mentioned with allyl-supported ligand, but not with borohydrides complexes.<sup>26</sup> Since this Mg compound was serendipitously isolated and did not correspond to the main objectives of this study, it was not subjected to further characterization apart from XRD resolution.

$$\begin{array}{c} & & & \\ & &$$

**Scheme 7** Tentative synthesis of (**PyA**<sup>2</sup>)-yttrium complex using the B/A route. The resulting products in brackets were not isolated.

With neodymium, the reaction of  $Nd(BH_4)_3(THF)_3$  with 1 equiv. of  $PyAH^2$  and 0.5 equiv. of BEM in toluene yielded a microcrystalline powder, identified by elemental analysis as the mono-substituted heterobimetallic "ate" complex  $[(PyA^2)Nd(BH_4)_3]_2[Mg(THF)_6]$  ( $\mathbf{3}_{Nd}$ ) (Scheme 8, step (a)), as classically obtained using this synthetic route.<sup>23</sup> The <sup>1</sup>H NMR paramagnetic spectrum of  $\mathbf{3}_{Nd}$  in  $C_6D_6$  (Fig. S8, SI section†) was quite similar to that of the previously prepared mono-substituted complex  $\mathbf{1'}_{Nd}$  (Fig. S5, SI section†), which facilitated the identification of the peaks belonging to the  $PyA^2$  ligand coordinated to Nd. The integration of the peaks revealed a total of fifteen proton resonances, including that of the borohydride groups as a broad signal at  $\delta$  = 76.5 ppm integrating for 8H, and fourteen peaks remaining for the ligand.

Scheme 8 Synthesis of  $[(PyA^2)Nd(BH_4)_3]_2[Mg(THF)_6]$  (3<sub>Nd</sub>) and crystallization leading to  $(PyA^2)Nd(BH_4)_2(THF)_2$  (3'<sub>Nd</sub>).

Crystals suitable for XRD were obtained from a concentrated solution of  $\mathbf{3}_{Nd}$  in THF with a vapor of pentane, which was kept at -40 °C for several days (Scheme 8, step (b)). The molecular structure displayed a magnesium-free neodymium complex  $\mathbf{3'}_{Nd}$  (see Section 4, crystallography part). Meanwhile, the <sup>1</sup>H NMR spectrum of the crystals of  $\mathbf{3'}_{Nd}$  displayed the same set of paramagnetic resonances as observed for  $\mathbf{3}_{Nd}$ , confirming that the complex prepared in solution was of the form of the mono-substituted ( $\mathbf{PyA^2}$ )Nd(BH<sub>4</sub>)<sub>2</sub>(THF)<sub>2</sub> (Fig. S9, SI section).

#### 3.4. (PyA³)-supported complexes

The reaction of 1 equiv. of Y(BH<sub>4</sub>)<sub>3</sub>(THF)<sub>3</sub> with **PyAH**<sup>3</sup> and 0.5 equiv. of BEM failed to afford a clean (**PyA**<sup>3</sup>)-Y complex. Instead, crystallization attempts at low temperature resulted in the isolation of brown single crystals, which, after XRD analysis, revealed to be (**PyA**<sup>3</sup>)Mg(BH<sub>4</sub>)(THF), lacking yttrium, as already observed with **PyA**<sup>2</sup> ligand. As same as previously discussed, this (**PyA**<sup>3</sup>)-Mg derivative coud result from Y/Mg **PyA**<sup>3</sup> ligand exchange during the crystallisation process (Scheme 9, top). At this stage, this complex was not subjected to further characterization, with the exception of XRD analysis (see Fig. S15, SI section†).

Mixing 1 equiv. of  $Y(BH_4)_3(THF)_3$  and **PyAH**<sup>3</sup> in THF at room temperature followed by the addition of <sup>n</sup>BuLi (Scheme 9, bottom) resulted in the deprotonation not only of the amino group but also of the

imine methyl substituent, leading to a dianionic amido/ene-amido ligand PyA(EA), which yielded, after recrystalization in toluene/pentane, single crystals of an yttrium complex of the form  $[(PyA(EA))Y(BH_4)_2][Li(THF)_4]$  ( $S_Y$ ) (see Section 4, crystallography part and  $^1H$  NMR spectra, Figs. S10-11, as well as  $^{13}C$  NMR in  $C_6D_6$ , Fig. S12, SI section $^+$ ). Deprotonation of the imine methyl proton of a related bidentate imino-pyridine ligand (Chart 1:  $PyIm^1$ ) has been reported in the literature, leading to the subsequent formation of the ene-lithium amide complex.  $^{27}$ 

Scheme 9 Formation of (PyA<sup>3</sup>)-Mg supported compound from the reaction of Y(BH<sub>4</sub>)<sub>3</sub>(THF)<sub>3</sub>/PyAH<sup>3</sup> with 0.5 equiv. of BEM and of  $[(PyA(EA))Y(BH_4)_2][Li(THF)_4]$  (5<sub>Y</sub>) from the reaction with 1 equiv. of <sup>n</sup>BuLi

With Nd, the reaction of Nd(BH<sub>4</sub>)<sub>3</sub>(THF)<sub>3</sub> with **PyAH**<sup>3</sup> and 0.5 equiv. of BEM was performed in the bulk according to Scheme 10. The  $^1$ H NMR spectrum of the crude product revealed a set of sixteen paramagnetic peaks ranging from -20 to 100 ppm, among which the broad resonance at  $\delta$  = 62 ppm integrating for 8 H was attributed to the BH<sub>4</sub> groups (Fig S13, SI section†). Elemental analysis was found consistent with the molecular formula (**PyA**<sup>3</sup>)Nd(BH<sub>4</sub>)<sub>2</sub> (**4**<sub>Nd</sub>) with an additional THF molecule. X-ray quality red crystals were obtained from standing a toluene solution of **4**<sub>Nd</sub> for a couple of days at room temperature. The molecular structure (**PyA**<sup>3</sup>)Nd(BH<sub>4</sub>)<sub>2</sub> was further confirmed by XRD analysis for that complex **4**<sub>Nd</sub> (see Section 4, crystallography part).

Scheme 10 Bulk synthesis of amido-imino pyridine neodymium complex 4<sub>Nd</sub>.

#### 4. X-ray structure analyses of organometallic complexes

The molecular structure of  $\mathbf{1}_Y$  is depicted in Fig. 3, with selected bond distances and angles listed in Table 2. Complex  $\mathbf{1}_Y$  crystallizes in the P-1 space group and its molecular structure exhibits an ionic pair consisting of two anionic yttrium units, each bearing one ligand  $\mathbf{PyA^1}$  as well as three BH<sub>4</sub>, along with a magnesium THF adduct of oxidation +2 as a counter-cation. The geometry at the Y center in  $\mathbf{1}_Y$  can be best described as an intermediate between a distorted square-based pyramid and a trigonal-based

bipyramid with  $\tau = 0.46.^{28}$  The bond lengths between the N(Pyr) atom of the chelating ligand **PyA¹** and Y [N1-Y = 2.460(2) Å] as well as the N(amido) atom and yttrium [N2-Y = 2.205(2) Å] of complex  $\mathbf{1}_Y$  are very close to that found in related bis-chelated amidopyridine yttrium amido complexes {[2-(RNCH<sub>2</sub>)-C<sub>5</sub>H<sub>4</sub>N]<sub>2</sub>YN(SiMe<sub>3</sub>)<sub>2</sub> with R =  $^t$ Bu or 2,6- $^i$ Pr<sub>2</sub>C<sub>6</sub>H<sub>3</sub>; N(Pyr)-Y = 2.433 – 2.484 Å and N(amido)-Y = 2.231 – 2.248 Å}. <sup>12a</sup> In this complex, two borohydrides are placed in a typical distance range for a tri-hapto coordination mode [Y-B1 = 2.550(3) Å, Y-B3 = 2.534(4) Å] and one in a di-hapto mode [Y-B2 = 2.780(3) Å], <sup>29</sup> with no solvent coordinated to the metal center. Additional information regarding the structural description of  $\mathbf{1}_Y$  can be found in the SI section (Table S2).

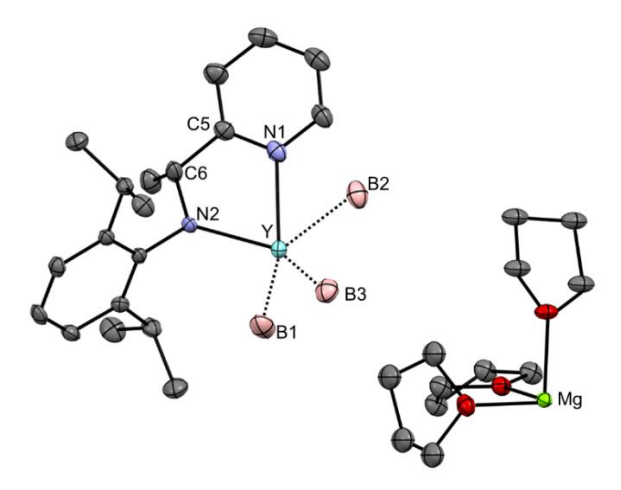
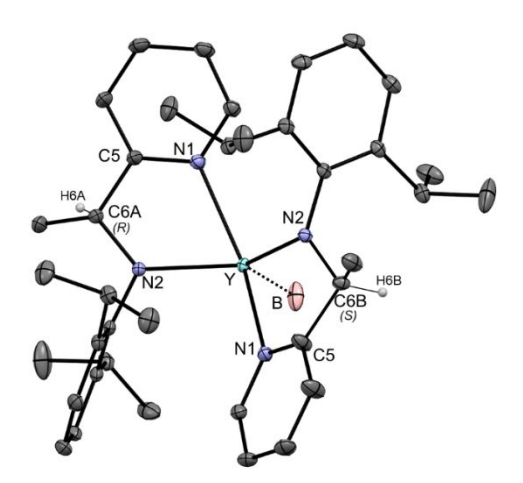


Fig. 3 Molecular structure of sub-unit  $[(PyA^1)Y(BH_4)_3]\{[Mg(THF)_6]\}_{0.5}$  of mono-substituted borohydride  $\mathbf{1}_Y$ . Hydrogens omitted for more clarity. Thermal ellipsoids are drawn at the 30% probability level.

The molecular structure of complex  $\mathbf{2}_{Y}$  is displayed in Fig. 4, with selected bond distances and angles listed in Table 2. Complex  $\mathbf{2}_{Y}$  crystallized in the C2/c space group, just like its neodymium analog  $\mathbf{2}_{Nd}$  (vide infra). The molecular structure of complex  $\mathbf{2}_{Y}$  presents a penta-coordinated yttrium center bound by two  $\mathbf{PyA^1}$  ligands and one borohydride group. The absolute configuration of the chiral carbon C6 on the ligand  $\mathbf{PyA^1}$  could not be distinguished due to the presence of disorder in  $\mathbf{2}_{Y}$ , which results in carbon splitting into C6a and C6b in a ratio of 0.587(2) and 0.413(2), respectively. The geometry of  $\mathbf{2}_{Y}$  can be seen, as in  $\mathbf{1}_{Y}$ , as an intermediate between a distorted square-based pyramid and a trigonal-based bipyramid with  $\tau = 0.47$ . The N(amido)-Y [N1-Y = 2.2147(10) Å] bond distance is equivalent for both  $\mathbf{PyA^1}$  chelates as well as the N(Pyr)-Y bond length [N2-Y = 2.4363(10) Å], which are similar to those found in complex  $\mathbf{1}_{Y}$  [N(amido)-Y = 2.205(2) and N(Pyr)-Y = 2.460(2) Å]. With a Y-B distance of 2.531(2) Å, the length is in the typical range for a BH<sub>4</sub> coordination in the tri-hapto mode.<sup>29</sup> The N-aryl plane and the pyridine ring are *quasi* orthogonal to each other with an angle of 85.96(5)°. Additional information regarding the structural description of  $\mathbf{2}_{Y}$  can be found in the SI section (Table S2).



**Fig. 4** Molecular structure of  $(PyA^1)_2Y(BH_4)$   $(2_Y)$  with illustration of the C6a and C6b carbon atoms that have been fixed with the (R) and (S) configurations, respectively, on the  $PyA^1$  ligands. Hydrogens have been omitted for clarity apart from the hydrogen H6a and H6b. Thermal ellipsoids are drawn at the 30% probability level.

The molecular structure of  $\mathbf{1''}_{Nd}$  exhibits a neutral dimeric complex, with two neodymium each bound to a  $PyA^1$  ligand (one (R) ligand on one Nd, (S) on the other) and a borohydride group, along with two BH<sub>4</sub> bridged between the two metals (Fig. 5). Crystallizing in the P2<sub>1</sub>/n group, the geometry at the Nd center can be best described as a distorted octahedron, with B1 and N1 atoms in the axial position [B1-Nd-N1 = 172.9(2)°]. The B1-Nd distance of 2.641(8) Å is within the expected range for a terminal  $\eta^3$  coordination of the borohydride, while the B2-Nd distance of 2.985(7) Å [and B2-Nd' of 2.923(7) Å] is slightly longer than usual for a bridging coordination mode.<sup>30</sup> As expected, the N(amido)-Nd bond [Nd-N2 = 2.260(5) Å] is shorter than the N(Pyr)-Nd bond distance [Nd-N1 = 2.578(4) Å]. To the best of our knowledge,  $\mathbf{1''}_{Nd}$  is the first example of a homo-bimetallic neodymium complex that bears both a terminal borohydride group and a bridged borohydride ligand. Additional information regarding the structural description of  $\mathbf{1''}_{Nd}$  can be found in the SI section (Table S2).

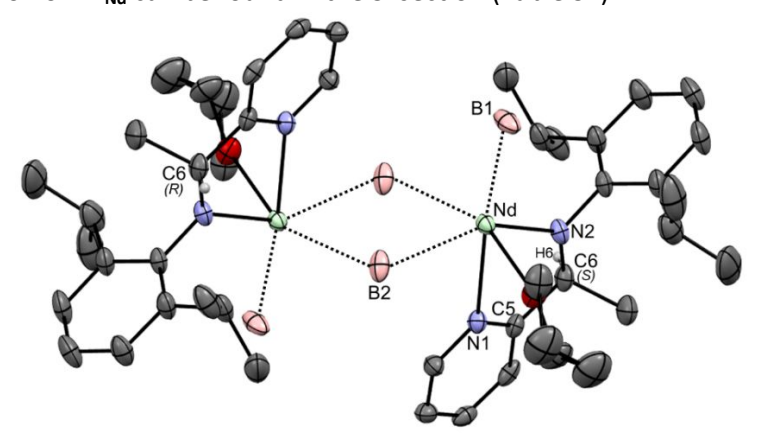


Fig. 5 Molecular structure of  $[(PyA^1)Nd(BH_4)(\mu-BH_4)(THF)]_2$  (1"<sub>Nd</sub>), the hydrogen atoms have been partially omitted for clarity, except the hydrogen H6. Thermal ellipsoids are drawn at the 30% probability level.

Complex  $\mathbf{2}_{Nd}$  crystallizes in the C2/c space group (Fig. 6), forming a neutral Nd complex comprising two  $\mathbf{PyA^1}$  ligands and one  $\mathbf{BH_4}$  group. The N(Pyr) of the  $\mathbf{PyA^1}$  ligands, as well as the N(amido) atoms, are arranged in *trans* configuration relative to each other. As in  $\mathbf{2}_{Y}$ , the chiral C6 carbon of the  $\mathbf{PyA^1}$  ligand is disordered in a ratio of 0.559(5) for C6a and 0.441(5) for C6b. In complex  $\mathbf{2}_{Nd}$ , the structure shows

the two ligands at the same distance from the neodymium center with the Nd-N1(Pyr) = Nd-N1'(Pyr) = 2.5488(10) Å being, as usual, longer than the Nd-N2(amido) = Nd-N2'(amido) = 2.2824(10) Å bond distances. Both distances show that the ligands are approximately 0.1 Å further from neodymium than from yttrium in complex  $\mathbf{2}_{Y}$ . This observation is consistent with the difference in the crystalline ionic radius of these elements for  $Y^{3+}$  and  $Nd^{3+}$  (CN = 8).<sup>31</sup> The Nd-B distance of 2.648(2) Å, in a classical range for a tri-hapto BH<sub>4</sub> coordination mode, completes the coordination sphere without additional solvent molecule. Additional information regarding the structural description of  $\mathbf{2}_{Nd}$  can be found in the SI section (Table S2).

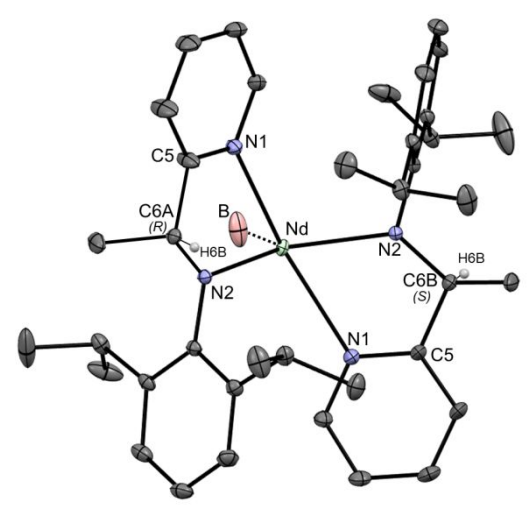


Fig. 6 View of the molecular structure of (PyA¹)<sub>2</sub>Nd(BH<sub>4</sub>) (2<sub>Nd</sub>), with representation of the C6a and C6b carbon atoms that have been respectively immobilized with the (R) and (S) configurations on the PyA¹ ligands. Hydrogen atoms have been omitted for clarity apart from the hydrogen H6a and H6b. Thermal ellipsoids are drawn at the 30% probability level.

<b>Table 2</b> Selected bo	ond distances and	l angles for	( <b>PyA¹</b> )-compl	lexes <b>1</b> <sub>Y</sub> , <b>2</b> <sub>Y</sub> , <b>1"</b> <sub>Nd</sub> :	and <b>2<sub>Nd</sub></b>
----------------------------	-------------------	--------------	-----------------------	---	---------------------------

	1 <sub>Y</sub>	<b>2</b> <sub>Y</sub>	1" <sub>Nd</sub>	2 <sub>Nd</sub>
MB1 (Å)	2.550(3)	2.531(2)	2.641(8)	2.648(2)
MB3 (Å)	2.534(4)			
MB2 (Å)	2.780(3)	n.a.	2.985(7)	n.a.
M'B2 (Å)			2.923(7)	
M-N(Pyr) (Å)	2.460(2)	2.4363(10)	2.578(4)	2.5488(10)
M-N(amido) (Å)	2.205(2)	2.2147(10)	2.260(5)	2.2824(10)
Twist angles	14.0(4)	PyA <sup>1(5)</sup> : 32.8(3)	2.2/7)	PyA <sup>1(S)</sup> : 11.0(3)
Pyr/Amido (°)	14.9(4)	PyA <sup>1(R)</sup> : -12.5(3)	3.3(7)	PyA <sup>1(R)</sup> : -31.2(4)
Pyr <i>vs.</i> Aryl plan (°)	68.95(9)	85.96(5)	74.9(2)	85.58(5)

Substituting  $PyA^1$  with  $PyA^2$  ligand led to notable structural diversity when coordinated to Nd. Complex  $3'_{Nd}$  crystallizes in the space group  $P2_1/c$  as a neutral mono-substituted bis-borohydride neodymium complex, with two THF molecules completing the coordination sphere (Fig. 7). Selected bond distances and angles are listed in Table 3. The geometry can be best described as a distorted octahedron, with the longest bond being Nd-O1 = 2.6924(9) Å. The THF molecule occupies-the axial position with respect to the N2(amido) atom [N2-Nd1-O1 =  $176.38(3)^\circ$ ], while N1, O2, B1 and B2 define the equatorial plane. The N(Pyr) and N(amido) bond lengths are similar to those found in  $2_{Nd}$  [ $2_{Nd}$ : N1-Nd = 2.5488(10) Å, N2-Nd = 2.2824(10) Å vs.  $3'_{Nd}$ : N1-Nd = 2.567(10) Å, N2-Nd = 2.2999(9) Å]. Both borohydrides exhibit a

tri-hapto coordination mode [Nd-B1 = 2.6829(15) Nd-B2= 2.6818(15) Å], comparable to the Nd-B distance in  $\mathbf{2}_{Nd}$ . Additional structural details of  $\mathbf{3'}_{Nd}$  can be found in the SI section (Table S3).

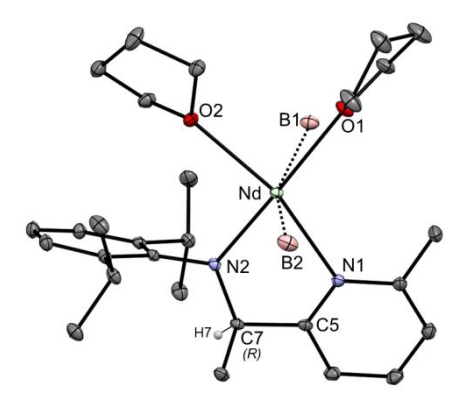


**Fig. 7** Representation of the molecular structure of magnesium-free (**PyA**<sup>2</sup>)Nd(BH<sub>4</sub>)<sub>2</sub>(THF)<sub>2</sub> (**3'**<sub>Nd</sub>) with ligand **PyA**<sup>2(R)</sup>, hydrogen atoms have been omitted for more clarity apart from H7. Thermal ellipsoids are drawn at the 30% probability level.

The XRD analysis of crystals of  $\bf 5_Y$  revealed an ionic pair comprising the anionic  $[(PyA(EA))Y(BH_4)_2]$  moiety associated with the  $[Li(THF)_4]$  cation, which crystalized in the C2/c space group (Fig. 8, Table 3). The yttrium center is coordinated to three N atoms from the ligand and two BH<sub>4</sub> groups in a  $\eta^3$  mode [Y-B1=2.537(2) Å and Y-B2 = 2.548(2) Å)], and exhibits a distorted square-based pyramidal geometry with  $\tau=0.33$ . The C13-N1 bond length of 1.379(2) Å is much longer than typical for a C(sp2)-N bond  $[e.g.\ C(sp2)-N\ bond\ distances$  in  $(PyA^3)$ -Mg supported complex and  $\bf 4_{Nd}\ (vide\ infra)$  are 1.284(2) Å and 1.281(4) Å, respectively], which can be identified as a single C-N bond. This is supported by the short C14-C13 bond length of 1.355(2) Å, characteristic of C(sp2)-C(sp2) bond distances, confirming the deprotonation of the imine methyl substituent to form an ene-amido group. The N(ene-amido)-Y bond length  $[N1-Y=2.336(1)\ Å]$  is longer than the N(amido)-Y bond distance  $[N3-Y=2.253(1)\ Å]$ , both of them being shorter than the N(Pyr)-Y  $[N2-Y=2.400(1)\ Å]$ . Additional structural description of  $\bf 5_Y$  can be found in the SI section (Table S3).

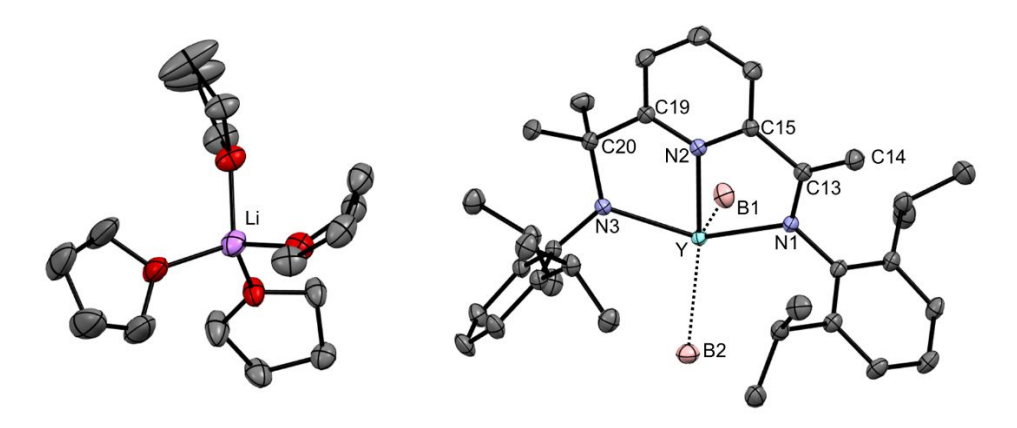


Fig. 8 Molecular structure of  $[(PyA(EA))Y(BH_4)_2][Li(THF)_4]$  (5<sub>Y</sub>), with the hydrogen atoms omitted for clarity. Thermal ellipsoids are drawn at the 30% probability level.

The X-ray structure of  $4_{Nd}$  showed a neutral Nd species supported by one ligand and two borohydride groups, which crystallized in the P2<sub>1</sub>/c space group (Fig. 9, Table 3). The Nd center adopts a highly distorted square-based pyramidal geometry, with  $\tau = 0.33$ . The two distances Nd-B1 = 2.593(5) Å and Nd-B2 = 2.611(3) Å are in classic range for the  $\eta^3$  coordination mode. The imine [C13-N1 = 1.281(4) Å]

and the amido [C20-N3 = 1.490(4) Å] bond lengths are comparable to those in bis(alkyl) Lu<sup>8</sup> and Sc<sup>9d</sup> complexes bearing the same  $PyA^3$  ligand [C-N(imine) = 1.29 – 1.31 Å, C-N(amido) = 1.47 – 1.48 Å]. The N(Py)-Nd [N2-Nd = 2.512(3) Å] and N(amido)-Nd [N3-Nd = 2.257(2) Å] bond distances are similar to those found in complexes  $2_{Nd}$  and  $3'_{Nd}$ . The N(imine)-Nd [N1-Nd = 2.616(3) Å] distance falls within the normal range when compared to related structure found in the literature.<sup>33</sup> Additional structural description of  $4_{Nd}$  is provided in the SI section (Table S3).

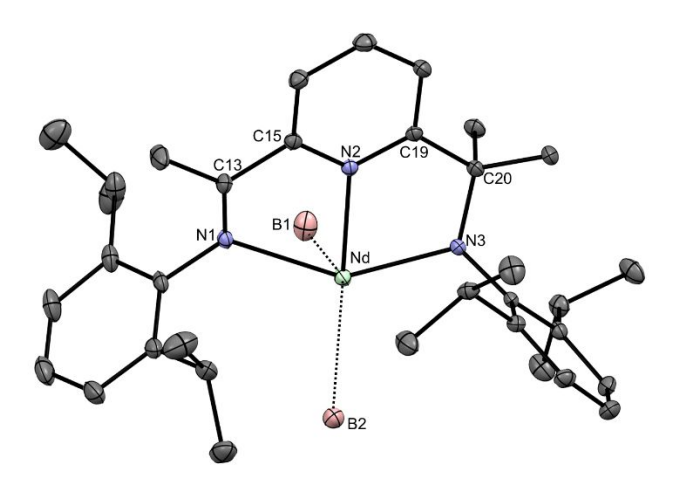


Fig. 9 Molecular structure of  $(PyA^3)Nd(BH_4)_2$   $(4_{Nd})$ , hydrogen omitted for more clarity. Thermal ellipsoids are drawn at the 30% probability level.

	3′ <sub>Nd</sub>	5 <sub>Y</sub>	4 <sub>Nd</sub>
MB1 (Å)	2.6829(15)	2.537(2)	2.593(5)
MB2 (Å)	2.6818(15)	2.548(2)	2.611(5)
M-N(Pyr) (Å)	2.567(10)	2.400(1)	2.512(3)
M-N(amido) (Å)	2.2999(9)	2.253(1)	2.257(2)
M-N(imine) (Å)	n.a.	2.336(1) [N(ene-amido)]	2.616(3)
Twist angles Pyr/amido (°)	18.90(14)	16.3(2)	-24.1(3)
Pyr/imine (°)	n.a.	5.9(2) [N(ene-amido)]	-1.3(4)
Pyr vs. N(amido)-aryl plan (°)	69.19(14)	88.5(2)	91.22(9)
Pvr vs N(imine)-arvl plan (°)	n a	70 5(2) [N(ene-amido)]	80 53(12)

Table 3 Selected bond distances and angles for (PyA<sup>2</sup>)- and (PyA<sup>3</sup>)- complexes 3'<sub>Nd</sub>, 5<sub>Y</sub> and 4<sub>Nd</sub>

#### 5. Polymerization reactions

A large number of rare-earth borohydride complexes have been investigated for their ability to catalyze the ring-opening polymerization (ROP) of lactone and lactide, to afford biodegradable and biocompatible polymers.<sup>6f,34</sup> The polymerization mechanism that takes place occurs through coordination-insertion, as was established more than two decades ago.<sup>35</sup> In the particular case where the initiator bears a BH<sub>4</sub> ligand, this will lead to different chain-end functions in the produced polyester, either hydroxy or formyl end-group.<sup>36</sup> The first mention of a rare-earth complex involving a borohydrido initiating group for ROP was reported nearly twenty years ago by S. Guillaume *et al.*<sup>37</sup> Since then, many complexes of that kind have been studied for this polymerization of cyclic esters, with TOF values at room temperature reaching up to 14 000 (lactide) and 700 000 h<sup>-1</sup> (ε-caprolactone).<sup>38,25a,b</sup> Among them, our group described the synthesis of mixed rare-earth complexes containing both borohydride/allyl reactive groups. DFT studies and polymer chain-end analysis

confirmed that the ring-opening polymerization using these mixed complexes was initiated by the borohydride moiety,  $^{25c}$  following the previously described process by Guillaume and colleagues. Some of the borohydride complexes prepared in the present work were thus preliminary evaluated in the ROP of cyclic esters:  $[(\mathbf{PyA^1})Y(\mathbf{BH_4})_3]_2Mg(\mathbf{THF})_6$   $(\mathbf{1_Y})$ ,  $[(\mathbf{PyA^1})Nd(\mathbf{BH_4})_2.(\mathbf{BH_4})Mg(\mathbf{PyA^1})](\mathbf{THF})_4$   $(\mathbf{1_{Nd}})$  and  $(\mathbf{PyA^3})Nd(\mathbf{BH_4})_2$   $(\mathbf{4_{Nd}})$ . Table 4 gathers the results obtained for the ROP of L-lactide (L-LA) and rac-lactide (rac-LA). The SEC traces of isolated polylactides and an example of  $^1H$  NMR spectrum are included in the SI section† (Figs S16 and S18, respectively).

Table 4. Polymerization of lactide using 2-pyridinemethanamino Nd and Y complexes

Entry a)	Metal catalyst (M = Nd, Y)	<i>L</i> -LA	Time	Conv.	TOF d)	$\overline{M}_{n(th)}$	$\overline{M}_{n(exp)}$	Đ	N g)
		(eq/M) b)	(min)	(%) <sup>c)</sup>		(g/mol) e)	(g/mol) f)		IN 87
<b>1</b> h)	Nd(BH <sub>4</sub> ) <sub>3</sub> (THF) <sub>3</sub>	100	90	0	0	-	-	-	
2	1 <sub>Nd</sub>	200	5	98	2350	28 300	26 400	1.5	1.1
3	1 <sub>Nd</sub>	400	10	52	1250	30 000	25 500	1.5	1.2
<b>4</b> i)	<b>1</b> <sub>Y</sub>	500	60	98	490	41 800	53500	2.0	0.8
<b>5</b> <sup>j)</sup>	1 <sub>Nd</sub>	250	40	99	371	35 600	13 500	1.7	2.6
<b>6</b> <sup>j)</sup>	1 <sub>Nd</sub>	1 000	960	97	162	139 700	29 600	3.0	4.7
<b>7</b> j)	4 <sub>Nd</sub>	250	35	99	424	35 600	8 800	1.4	4.0
<b>8</b> j)	4 <sub>Nd</sub>	1 000	180	93	310	133 900	26 800	1.4	5.0

<sup>&</sup>lt;sup>a)</sup> Reaction conducted at room temperature in toluene, [L-LA] = 0.67 M; <sup>b)</sup> M = Nd, Y; <sup>c)</sup> conversion was determined by integration of the methine resonances by <sup>1</sup>H NMR; <sup>d)</sup> mol(monomer).mol(catalyst)-<sup>1</sup>(h)-<sup>1</sup>; <sup>e)</sup> calculated for one polymer chain per metal:  $\overline{M}_{n(th)} = [L-LA]_0$  /  $[Cat] \times conversion \times (molecular weight of <math>L-LA$ ); <sup>f)</sup> SEC analysis calibrated versus polystyrene standards,  $\overline{M}_{n(exp)} = \overline{M}_{nSEC(raw)} \times 0.58$ ; <sup>g)</sup> N chains per catalyst =  $\overline{M}_{n(th)}$  /  $\overline{M}_{n(exp)}$ ; <sup>h)</sup> [L-LA] = 0.33 M; <sup>i)</sup> reaction conducted at 50 °C; <sup>j)</sup> Reaction conducted at 50 °C in THF, [rac-LA] = 1 M.

With  $[(PyA^1)Nd(BH_4)_2.(BH_4)Mg(PyA^1)](THF)_4$  (1<sub>Nd</sub>), good-level activity in ROP of L-LA was noticed in toluene at room temperature (entries 2, 3), as compared to the literature for other very active rareearth initiators.<sup>25,34,38</sup> The impact of the **PyA**<sup>1</sup> ligand in the coordination sphere of the metal was here clearly noted, as Nd(BH<sub>4</sub>)<sub>3</sub>(THF)<sub>3</sub> failed to polymerize lactide under the same conditions at room temperature (entry 1). Nevertheless, we could not determine the influence of the Mg moiety within 1<sub>Nd</sub> toward the polymerization of cyclic ester. Molecular weights agreed well with one growing chain per metal and dispersity was found rather narrow (entries 2, 3). Polymerization using (PyA¹)-supported yttrium  $\mathbf{1}_{Y}$  in toluene exhibited a lower activity towards lactide than its neodymium counterpart  $\mathbf{1}_{Nd}$ , although being conducted at 50 °C (TOF<sub>1A</sub> = 490 vs. 1 250 h<sup>-1</sup>, entries 4 and 3, respectively), with almost one growing PLA chains per yttrium center (entry 4), as same as observed with  $\mathbf{1}_{Nd}$ . The broader dispersity when compared with that obtained with  $\mathbf{1}_{Nd}$  (2.0 vs. 1.5, entries 4 vs. 3, respectively) confirmed the lower control of the polymerization with this yttrium catalyst. In THF, at 50 °C (no polymerization occurred at room temperature), the activity was substantially reduced with catalyst  $\mathbf{1}_{Nd}$ (entries 5-6 vs. 2-3), likely due to the competition between THF and monomer coordination to the rareearth catalyst. However, unlike the reactions carried out in toluene, no gel formation was observed under these polymerization conditions. The switch from L-LA to rac-LA did not afford any selectivity in polymerization (entries 5-8). Regarding the molecular weights, smaller  $M_n$  values than expected were obtained in THF, speaking in favor of transfer reactions. Polymerization reactions conducted with  $(PyA^3)Nd(BH_4)_2$   $(4_{Nd})$  appeared to be faster than with  $1_{Nd}$  (entries 7-8 vs. 5-6, respectively) and the experimental molar masses were of the same magnitude order with both catalysts, with 3-5 polymer chains per metal. This confirmed the occurrence of transfer side-reactions as two chains were to be expected considering a mono-substituted complex bearing two  $BH_4$  initiating groups. This latter catalyst allowed narrower dispersity than with  $\mathbf{1}_{Nd}$  and  $\mathbf{1}_{Y}$ .

Table 5. Polymerization of ε-caprolactone using 2-pyridinemethanamino Y and Nd complexes

Entry a)	Metal catalyst (M = Nd, Y)	CL	Time	Conv.	TOF d)	$\overline{M}_{n_{(th)}}$	$\overline{M}_{n_{(exp)}}$	Đ	N g)
		(eq/M) b)	(min)	(%) <sup>c)</sup>		(g/mol) e)	(g/mol) f)		N Si
9	1 <sub>Nd</sub>	200	< 1	98	11 800	22 300	15 600	1.8	1.4
10	1 <sub>Nd</sub>	1 000	< 5	98	11 800	111 700	28 400	1.4	3.9
11	1 <sub>Y</sub>	1 000	10	56	3 400	63 800	70 300	1.7	0.9
12 h)	1 <sub>Nd</sub>	250	1	73	10 900	20 800	8 200	1.3	2.5
13 h)	1 <sub>Nd</sub>	1 000	30	75	1 500	85 500	18 700	1.3	4.6
<b>14</b> h)	4 <sub>Nd</sub>	250	1	81	12 100	23 100	11 500	1.3	2.0
<b>15</b> h)	4 <sub>Nd</sub>	1 000	180	-	-	-	_	-	-

<sup>&</sup>lt;sup>a)</sup> Reaction conducted with  $10^{-3}$  mmol of catalyst at room temperature in toluene, [CL] = 0.67 M; <sup>b)</sup> M = Nd, Y; <sup>c)</sup> conversion was determined according to the yield by gravimetry; <sup>d)</sup> mol(monomer).mol(catalyst)<sup>-1</sup>(h)<sup>-1</sup>; <sup>e)</sup> calculated for one polymer chain per metal:  $\overline{M}_{n_{\text{(th)}}} = [\text{CL}]_0$  / [Cat] × conversion × (molecular weight of CL); <sup>f)</sup> SEC analysis calibrated versus polystyrene standards,  $\overline{M}_{n_{\text{(exp)}}} = \overline{M}_{n_{\text{SEC(raw)}}} \times 0.56$ ; <sup>g)</sup> N chains per catalyst =  $\overline{M}_{n_{\text{(th)}}}$  /  $\overline{M}_{n_{\text{(exp)}}}$ ; <sup>h)</sup> Reaction conducted in THF at room temperature with 5.10<sup>-3</sup> mmol catalyst and [CL] = 1 M.

The results of polymerizations of  $\varepsilon$ -caprolactone (CL) are gathered in Table 5. The SEC traces of isolated PCLs and an example of <sup>1</sup>H NMR spectrum are included in the SI section<sup>†</sup> (Figs S17 and S19, respectively). (PyA¹)-supported neodymium complex 1<sub>Nd</sub> displayed high activity in toluene (entries 9, 10) (TOF<sub>CL</sub> = 11 800 h<sup>-1</sup>). At low [m]/[M] ratio (entry 9, m = monomer, M = metal), 1.4 polymer chain was produced per metal. At high [m]/[M] ratio however, entry 10, a much higher number of polymer chains than expected was initiated, as already reported under such ratio conditions (see references below). By comparison, lower activity was noted with  $\mathbf{1}_{Y}$  (entry 11), but the polymerization was better controlled, with almost one polymer chain initiated per yttrium, as already observed with lactide polymerization with the same catalyst (entry 4, table 4). In THF, similar behaviour to that observed in toluene was found for  $\mathbf{1}_{Nd}$ , although the activity in ROP was slightly lower (entries 12, 13). The corresponding observed deviation in  $\overline{M}_{n(exo)}$  value (and thus the extra number of growing chains) may be explained as frequently justified by intramolecular (back-biting) and/or intermolecular transesterifications, 34,37b,39 leading to a mixture of cyclic and linear polymers. With (PyA3)-supported  $\mathbf{4}_{Nd}$  in THF at room temperature (solubility of  $\mathbf{4}_{Nd}$  in toluene was found too low), CL polymerization was rather efficient at low monomer to catalyst ratio (entry 14), while an increase in monomer quantity failed to produce some polymer (entry 15). Noteworthy is the good match between the experimental and theoretical  $\overline{M}_{
m n}$  values considering two polymer chains initiated per metal catalyst, in full agreement with the presence of two potential initiating groups in 4<sub>Nd</sub> (entry 14). In that case, in addition to the monomer/THF competition for neodymium coordination, the presence of the bulky **PyA<sup>3</sup>** ligand might prevent uncontrolled transesterification reactions.

#### 6. Conclusion

In summary, the synthesis of borohydride rare-earth complexes using 2-pyridinemethanamido ligands is drastically depending on the nature of the rare-earth, but also of different experimental conditions such as the solvent (THF or toluene) that may or not allow for better ligand exchange and the metal base (magnesium or lithium) used, which can leave the metal counterpart in the final structure of the isolated products. These complexes can either crystallize and confirm the substitution degree, as identified by elemental analysis, as neutral bis-substituted complexes ( $\mathbf{2}_{Nd}$ ,  $\mathbf{2}_{Y}$ ), mono-substituted ion

pair complex  $(1_{Y})$  or neutral mono-substituted complex  $(4_{Nd})$ . However, rearrangement during crystallization may lead to a different degree of substitution than initially identified by elemental analysis, as exemplified with neodymium. Indeed, crystallization of the ionic  $[(PyA^2)Nd(BH_4)_3]_2[Mg(THF)_6]$  (3<sub>Nd</sub>) results to the formation of the neutral complex 3'<sub>Nd</sub> and  $[(PyA^1)Nd(BH_4)(\mu-BH_4)(THF)]_2$  (1"Nd) is issued from ligands redistribution of  $1_{Nd}$ . In turn, all attempts to crystallize yttrium complexes with PyA2 and PyA3 ligands lead to the undesirable but interesting magnesium pyridinemethanamido-borohydride supported complexes. This entire study indicated that the ligand PyA1 was a particular case: it appeared to be at the steric hindrance limit to allow the formation of a stable bis-substituted derivatives, while addition of a small substituent on the pyridine ring in **PyA**<sup>2</sup> led to the formation and isolation of mono-substituted complex only. When Y(BH<sub>4</sub>)<sub>3</sub>(THF)<sub>3</sub> was reacted with PyA<sup>3</sup>H in the presence of <sup>n</sup>BuLi, a rare example of ene-amido complex was isolated. Preliminary ROP experiments were carried out: the mono-substituted complexes  $\mathbf{1}_{Nd}$ ,  $\mathbf{1}_{Y}$  and  $\mathbf{4}_{Nd}$  were found promisingly efficient towards ROP of lactide and  $\epsilon\text{-caprolactone}.$  The Nd catalysts exhibited higher activity (up to 12 000 h-1 in CL ROP for 4<sub>Nd</sub> and 2 350 h-1 in LA ROP for 1<sub>Nd</sub>), while the polymerization was well controlled with  $\mathbf{1}_{Y}$  (LA and CL) and  $\mathbf{4}_{Nd}$  (CL). A full study of cyclic esters polymerization by means of the herein described (PyA)-Y and Nd supported complexes will be published in the near future.

#### **Experimental**

General methods and materials: organometallic syntheses have been performed in air-free condition under argon and the resulting complexes have been stored in a dry solvent-free glovebox (Jacomex O<sub>2</sub> < 1ppm, H<sub>2</sub>O < 1ppm) under argon. Toluene, THF and pentane were purified through an alumina column (Mbraun, Mérignac, France), deoxygenated by freeze-pump-thaw method, and then stored over benzophenone sodium. Solvents were either transferred to the reaction flask by trap-to-trap condensation at cold temperature or distilled and stored on 4 Å molecular sieves in the glovebox before use. Organic compounds (6-bromo-2-picoline, 2-acetylpyridine, 2,6-diisopropylaniline, 2,6diacetylpyridine, N,N-dimethylacetamide), borohydride salts (potassium or sodium borohydride), acidic salts and bases [N,N-dimethylanilinium tetrakis(pentafluorophenyl)borate, KN(SiMe<sub>3</sub>)<sub>2</sub>, nbutyllithium (1.6 M in hexanes), methyllithium (1.6 M in THF)], monomers (lactide, L- and rac-, and εcaprolactone), rare-earth precursors (neodymium and yttrium tri-chloride) were acquired from Sigma-Aldrich, TCI or Fisher scientific. Butyl(ethyl)magnesium (1.28 M, in hexanes) was purchased from Texas alkyl. The organic compounds were used as received while the borohydride and acidic salts, bases and rare-earth precursors were stored before use in the glovebox. Lactide (L- and rac-) used for polymerization was purified by recrystallization twice from a hot solution in toluene and filtered after each crystallization to remove traces of residual lactic acid. The lactide was then sublimed under vacuum over P2O5 and then stored in the glovebox. E-caprolactone was dried under argon over CaH2 before trap-to-trap distillation and then stored at -20 °C in the glovebox.

2,6-diisopropylphenyl-1-(pyridin-2-yl)ethan-1-imine ( $PyIm^1$ ), <sup>18a</sup> 2,6-diisopropyl-1-(pyridin-2-yl)ethyl)aniline ( $PyAH^1$ ), <sup>18a</sup> 2,6-diisopropylphenyl-1-(6-methylpyridin-2-yl)ethan-1-imine ( $PyIm^2$ ), <sup>4</sup> 2,6-diisopropylphenyl-1-(6-methylpyridin-2-yl)ethyl)aniline ( $PyAH^2$ ), <sup>4</sup> 1,1'-(pyridine-2,6-diyl)bis(2,6-diisopropylphenyl)ethan-1-imine) ( $PyIm^3$ ), <sup>18c</sup> (1-(6-(2-((2,6-diisopropylphenyl)amino)propan-2-yl)pyridin-2-yl)ethylidene)-2,6-diisopropylaniline ( $PyAH^3$ ), <sup>18b</sup> ( $PyAH^3$ ),

<sup>1</sup>H NMR spectra were recorded on a Brucker Advance 300 instrument at 300 K. <sup>1</sup>H chemical shifts (reported in ppm) were determined by using the residual signal of the deuterated solvent according to

the literature. Elemental analyses were performed on an Elementar Vario Cube apparatus at UCCS, University Lille Nord de France. For the polymers, the conversion was determined by mean of  $^1H$  NMR spectroscopy by using Topspin software. Size exclusion chromatography (SEC) analyses of the samples were performed in THF (+ 0.1 % toluene) as an eluant at 35 °C (1 mL/min) with an Agilent 1260 pump, a Wyatt Optilab refractometer, and Waters Styragel columns (HR1, HR3 and HR4) calibrated with polystyrene standards. The SEC profile was further retraced in MS Excel with calibration equation and the data were verified. The number-average molar mass values were corrected using the coefficient Y, according to  $\overline{M}_n = \overline{M}_{n \text{SEC(raw)}} \times \text{Y}$ , where Y = 0.58 for lactide and 0.56 for \$\varepsilon\$-caprolactone. \$^{42}\$

X-ray measurements for  $PyAH^2$ ,  $1_Y$ ,  $2_Y$ ,  $1''_{Nd}$ ,  $2_{Nd}$ ,  $3'_{Nd}$ ,  $4_{Nd}$ ,  $5_Y$  and the Mg-PyA¹ and Mg-PyA² supported complexes were conducted at a temperature of 100 K, using an Apex II DUO CCD 4K Bruker diffractometer with a wavelength ( $\lambda$ ) of 0.71073 Å. The crystal structures were determined using the SHELXT method,  $^{43}$  and subsequently, they were further refined through least-squares procedures based on F2 using SHELXL.  $^{44}$  X-ray measurement for  $KN(SiMe_3)_2$ .  $PyAH^1$  was performed on a Bruker SMART APEX II diffractometer. The APEX2 $^{45}$  program package was used to determine the unit-cell parameters and for data collection (10 sec/frame scan time for a sphere of diffraction data). The raw frame data was processed using SAINT $^{46}$  and SADABS $^{47}$  to yield the reflection data file. Bond distances and angles were determined using the Olex2 program,  $^{48}$  while the representation of each molecular structure was performed using the Mercury program.  $^{49}$  Detailed information regarding the refinement data can be found in the Tables S1, S2 and S3 in the supporting information.

AgNO<sub>3</sub> test: a few milligrams of the product were placed in a small flask and melted in the presence of potassium hydroxide to form a white foam. Water was then added, followed by a solution of concentrated HNO<sub>3</sub> to neutralize the pH giving a colorless solution. A few drops of a 1 M AgNO<sub>3</sub> solution were added, and the presence of chlorine was verified by the appearance of AgCl as a white precipitate. This test allowed to detect residual chloride traces in the compounds.

General polymerization reactions: a reactor was loaded with the desired equivalent of monomer (200, 250, 400, 500 or 1000 equiv.) and stirred in the solvent (THF or toluene) for 2 minutes. The catalyst was then added in the reactor and the reaction mixture was stirred either in an oil bath at 50 °C or at room temperature. Once the reaction was completed (after a given time or in case of any gel formation), the solution was quenched with a few drops of toluene containing a small amount of acidified water. An aliquot was collected to get the ¹H NMR conversion and the polymer was isolated by precipitation in a large volume of ethanol (250 mL) before being dried under *vacuum*.

#### <sup>1</sup>H NMR monitoring experiment.

Y(BH<sub>4</sub>)<sub>3</sub>(THF)<sub>3</sub> + 2 PyAH<sup>1</sup> + BEM (C<sub>6</sub>D<sub>6</sub>): the reagents (4.0 mg, 11.4 μmol; 6.4 mg, 22.8 μmol; 8.8 μL, 11.4 μmol, respectively) were weighed in an NMR tube equipped with a teflon valve and 0.4 mL of solvent (THF-D<sub>8</sub>) was added. The <sup>1</sup>H NMR spectrum recorded immediately is shown in SI section<sup>†</sup>, Fig. S2b.

#### Syntheses.

**Preparation of KN(SiMe<sub>3</sub>)<sub>2</sub>.PyAH¹ adduct.** In a dried Schlenk tube, to a solution of **PyAH¹** (0.208 g, 0.74 mmol) in THF was added KN(SiMe<sub>3</sub>)<sub>2</sub> (0.147 g, 0.74 mmol). The yellow starting solution was left under stirring overnight to turn dark brown. Evaporation, filtration in toluene and *vacuum* drying yielded a dark brown powder. The powder was dissolved in the minimum amount of pentane and then left at -35 °C for crystallization. 0.193 g (0.40 mmol, 54%) of dark crystals suitable for XRD were obtained.  $^1$ H NMR (300 MHz, THF-D<sub>8</sub>, Fig. S1, SI section†):): δ (ppm) = -0.20 (br, 16H, SiCH<sub>3</sub>), 1.01 (d, 6H,  $^3$ J<sub>HH</sub> = 6.83 Hz, CH(CH<sub>3</sub>)<sub>2</sub>), 1.18 (d, 6H,  $^3$ J<sub>HH</sub> = 6.83 Hz, CH(CH<sub>3</sub>)<sub>2</sub>), 1.42 (d, 3H,  $^3$ J<sub>HH</sub> = 6.6 Hz, NH-CH(CH<sub>3</sub>)), 3.31 (sept., 2H,  $^3$ J<sub>HH</sub> = 7 Hz, CH(CH<sub>3</sub>)<sub>2</sub>), 4.14 (q, 1H, NH-CH + s, 1H, NH), 6.87 (m, 1H, *meta*-CH<sub>pyr</sub>), 6.96 (d, 2H, *meta*-

 $CH_{Aryl}$ ), 7.05 (m, 1H,  $CH_{pyr}$ ), 7.13 (m, 1H,  $CH_{pyr}$ ), 7.54 (m, 1H, para- $CH_{Aryl}$ ), 8.56 (m, 1H, ortho- $CH_{pyr}$ ). Anal. Calcd. for  $C_{25}H_{44}N_3Si_2K$ : C, 62.35; H, 9.14; N, 8.73. Found: C, 62.65; H, 8.80; N, 9.24.

Preparation of [(PyA¹)Y(BH<sub>4</sub>)<sub>3</sub>]·<sub>2</sub>[Mg(THF)<sub>6</sub>]²·{1<sub>γ</sub>}: a colorless solution of Y(BH<sub>4</sub>)<sub>3</sub>(THF)<sub>3</sub> (0.400 g, 1.14 mmol) and PyAH¹ (0.320 g, 1.14 mmol) in toluene was treated with an 1.28 M solution of BEM (0.440 mL, 0.57 mmol, 0.49 equiv.) to give a yellow solution with the presence of a white precipitate. This solution was left under stirring for 30 min. Evaporation of the solvents yielded a yellow foam. Toluene (15 mL) was then added, followed by filtration and evaporation to obtain a new yellow foamy solid which was triturated in pentane and washed twice with it to afford a light-yellow powdery solid (0.52 g, 0.81 mmol, 71%). Crystals suitable for XRD were obtained from a concentrated solution in THF/pentane at -40 °C. ¹H NMR (300 MHz,  $C_6D_6$ , Fig. S2a, SI section†): δ (ppm) = 1.21 (d, 6H,  $^3$ J<sub>HH</sub> = 6.6 Hz, CH( $CH_3$ )<sub>2</sub>), 1.26 (dd, 6H,  $^3$ J<sub>HH</sub> = 6.3 Hz, CH( $CH_3$ )<sub>2</sub>), 1.31 (d, 3H,  $^3$ J<sub>HH</sub> = 6.9 Hz, N-CH( $CH_3$ )), 3.51 (sep, 2H,  $^3$ J<sub>HH</sub> = 6.7 Hz, CH( $CH_3$ )<sub>2</sub>), 4.17 (sep, 2H,  $^3$ J<sub>HH</sub> = 6.7 Hz, CH( $CH_3$ )<sub>2</sub>), 4.63 (q, 1H,  $^3$ J<sub>HH</sub> = 6.3 Hz, N-CH), 6.36 (br. t, 1H,  $^3$ J<sub>HH</sub> = 6.8 Hz, *meta*-CH<sub>pyr</sub>), 6.59 (br. d, 1H,  $^3$ J<sub>HH</sub> = 8.0 Hz, *meta*-CH<sub>pyr</sub>), 6.82 (td, 1H,  $^3$ J<sub>HH</sub> = 7.5 Hz,  $^5$ J<sub>HH</sub> = 1.1 Hz, *para*-CH<sub>pyr</sub>), 8.66 (m, 1H, *ortho*-CH<sub>pyr</sub>). The peaks integrating for the borohydride function are certainly hidden by the CH<sub>3</sub> peaks and the aryl peak missing might be hidden by the  $^1$ H resonance of NMR solvent. The  $^{13}$ C NMR spectrum is displayed in Fig. S3, SI section†. Anal. calcd. for  $C_{62}$ H<sub>122</sub>B<sub>6</sub>MgN<sub>4</sub>O<sub>6</sub>Y<sub>2</sub>: C, 57.83; H, 9.56; N, 4.35. Found: C, 56.80; H, 9.31; N, 4.26.

Isolation of (PyA¹)<sub>2</sub>Y(BH<sub>4</sub>) (2<sub>Y</sub>) from the attempted preparation of (PyA¹)Y(BH<sub>4</sub>)<sub>2</sub>: a colorless solution composed of 0.4 g of Y(BH<sub>4</sub>)<sub>3</sub>(THF)<sub>3</sub> (1.14 mmol) and 0.32 g of PyAH¹ (1.14 mmol) in toluene was treated with a 1.6 M solution of MeLi in THF (0.70 mL, 1.12 mmol, 0.98 equiv.) and left to stir during 10 minutes. Evaporation of the solvent, filtration in toluene (20 mL) and drying under *vacuum* afforded the product as a yellow foam which was washed twice with pentane (2 x 10 mL) to yield a yellow powder. Crystallization from a concentrated solution in toluene with a pentane vapor and standing at -40 °C allowed the obtention of small crop of crystals suitable for XRD. The molecular structure revealed the formation of (PyA¹)<sub>2</sub>Y(BH<sub>4</sub>) (2<sub>Y</sub>). ¹H NMR (300 MHz, C<sub>6</sub>D<sub>6</sub>, Fig. S3 bottom, SI section†):  $\delta$  (ppm) = 0.29 (t,  ${}^3J_{HH}$ = 7.5 Hz), 0.62 (d,  ${}^3J_{HH}$ = 6.9 Hz), 0.66 (d,  ${}^3J_{HH}$ = 6.8 Hz), 1.10 (d,  ${}^3J_{HH}$ = 6.6 Hz), 1.15-1.37 (m), 1.62 (d), 1.68 (d), 1.72 (d), 1.79 (d), 2.10 (s), 3.39 (qt), 3.79 (qt), 3.94 (qt), 4.05 (qt), 4.18 (qt), 4.34 (m), 4.45 (m), 4.57 (m), 4.69 (qd), 4.89 (qd), 5.15 (qt), 6.2-7.4 (m). The ¹³C NMR spectrum is displayed in Fig. S4, SI section†.

**Preparation of [(PyA¹)Nd(BH₄)₂(THF)₂] (1'Nd):** Nd(BH₄)₃(THF)₃ (0.288 g, 0.71 mmol) and **PyAH¹** (0.2 g, 0.71 mmol) were weighed in a double neck round bottom flask, then 20 mL THF was *vacuum* transferred by trap to trap distillation. 0.5 equiv. BEM (0.28 mL, 0.35 mmol) was added and the resulting orange mixture was allowed to react at room temperature for 1 h. The solvents were evaporated and the crude solid was extracted with toluene (10 mL) overnight. After filtration and elimination of salts, the green-orange solution was evaporated to dryness to afford a green solid (m = 0.330 g, 77.8%). ¹H NMR (300 MHz,  $C_6D_6$ , Fig. S4, SI section†):  $\delta$  (ppm) = -50.2 (s, 1H), -28.4 (s, 3H), -12.8 (s, 3H), -6.1 (s, 1H), -2.2 (THF), 1.3 (THF), 3.8 (s, 1H), 4.7 (s, 1H), 5.3 (s, 3H), 6.0 (s, 1H), 8.9 (s, 1H), 9.3 (s, 1H), 11.5 (s, 3H), 20.3 (s, 1H), 20.7 (1H), 34.3 (s, 3H), 36.5 (br s, 1H), 70.1 (br, BH₄), 96.5 (br s, 1H). Anal. calcd. for  $C_{27}H_{49}B_2N_2NdO_2$ :  $C_{17}C$ 

**Preparation of [(PyA¹)Nd(BH4)3Mg(PyA¹)(THF)4] (1**Nd): to a solution of Nd(BH4)3(THF)3 (0.280 g, 0.69 mmol) and two equiv. of **PyAH¹** (0.400 g, 1.14 mmol) in toluene (10 mL) was added one equiv. of a 1.28 M BEM solution in hexane (0.44 mL, 0.69 mmol). The solution turned from light blue to green and was left to stir for 30 min at room temperature. After evaporation of the solvent, the green foam was extracted with 20 mL of toluene and evaporated to dryness to give the product as a green powder that was washed with pentane (2 x 10 mL) (0.460 g, 0.43 mmol, 63%).  $^{1}$ H NMR (300 MHz,  $^{2}$ C<sub>6</sub>D<sub>6</sub>, Fig. S5, SI

section†) is identical to  $\mathbf{1'}_{Nd}$  with  $\delta$  (ppm) = -50.5 (s, 1H), -28.4 (s, 3H), -12.8 (s, 3H), -6.2 (s, 1H), -0.1 (THF), 1.6 (THF), 4.0 (s, 1H), 4.9 (s, 1H), 5.4 (s, 3H), 5.9 (s, 1H), 9.2 (s, 1H), 9.3 (s, 1H), 11.7 (s, 3H), 20.4 (s, 1H), 20.7 (1H), 34.3 (s, 3H), 37.4 (br s, 1H), 63 (br, 4H, BH<sub>4</sub>), 97.2 (br s, 1H). Anal. calcd. for  $[(\mathbf{PyA^1})\mathrm{Nd}(\mathrm{BH_4})_3\mathrm{Mg}(\mathbf{PyA^1})(\mathrm{THF})_4]$ : C, 60.92; H, 8.91; N, 5.26. Found: C, 61.25; H, 8.61; N, 5.37. A small amount (ca. 50 mg) of crystals suitable for XRD, obtained at cold temperature from a toluene/pentane mixture, revealed after analysis the isolation of the mono-substituted complex  $[(\mathbf{PyA^1})\mathrm{Nd}(\mathrm{THF})(\mathrm{BH_4})(\mu-\mathrm{BH_4})]_2$  ( $\mathbf{1''}_{Nd}$ ) lacking Mg.  $^1$ H NMR (300 MHz,  $C_6D_6$ ) was identical to that of complex  $\mathbf{1'}_{Nd}$ . The NMR scale reaction of Nd(BH<sub>4</sub>)<sub>2</sub>( $C_3H_5$ )(THF)<sub>3</sub> (8.6 mg, 20  $\mu$ mol) with 1 equiv. **PyAH**<sup>1</sup> ligand (5.6 mg, 20  $\mu$ mol) resulted after smooth heating (5 min) with a hair-dryer to a green solution, which  $^1$ H NMR spectrum was identical to that of  $\mathbf{1_{Nd}}$ ,  $\mathbf{1'_{Nd}}$  and  $\mathbf{1''_{Nd}}$ .

Preparation of (PyA¹)<sub>2</sub>Nd(BH<sub>4</sub>) (2<sub>Nd</sub>): as in the synthesis of [(PyA¹)<sub>2</sub>Nd(BH<sub>4</sub>)][Mg(BH<sub>4</sub>)<sub>2</sub>], a solution of Nd(BH<sub>4</sub>)<sub>3</sub>(THF)<sub>3</sub> (0.220 g, 0.54 mmol) and 1.95 equiv. PyAH¹ (0.300 g, 1.06 mmol) in toluene (10 mL) was treated with a 1.6 M solution of MeLi in THF (0.66 mL, 1.06 mmol, 1.95 equiv.). The solution turned from light blue to green with apparition of a white precipitate and was left for stirring for 30 min at room temperature. After evaporation of the THF, the green foam was extracted with 10 mL of toluene and left at room temperature with a vapor of pentane for crystallization. After 24 h green crystals suitable for XRD were obtained (0.150 g, 0.2 mmol, 19%). The ¹H NMR spectrum (Fig. S6, SI section†) could not be interpreted due to paramagnetism of Nd, but it was very similar to that recorded in the case of an NMR-scale synthesis. We have made several attempts to obtain accurate elemental analysis results for this product, but our efforts have proved unsuccessful.

Preparation of [(PyA²)Nd(BH₄)₃]₂[Mg(THF)₆] (3<sub>Nd</sub>): to a blue solution of Nd(BH₄)₃(THF)₃ (0.300 g, 0.74 mmol) and 1 equiv. of PyAH² (0.220 g, 0.74 mmol) in toluene (10 mL) is added 0.5 equiv. of a 1.28 M BEM solution in hexane (0.29 mL, 0.37 mmol). The solution changed from light blue to green (with presence of a precipitate) and was left to stir for 1 h at room temperature. After evaporation of the solvent, the green foam was extracted with 20 mL of toluene and dried under *vacuum* to give the product as a green powder, which was washed with pentane (2 x 10 mL) (0.350 g, 0.57 mmol, 77%).  $^{1}$ H NMR (300 MHz, C₆D₆): δ (ppm) = -40.62 (s, 3H), -24.7 (s, 3H), -10.55 (s, 3H), -6.27 (s, 1H), 3.26 (s, 3H), 4.31 (s, 2H), 5.76 (s, 3H), 6.09 (s, 1H), 8.73 (s, 1H), 11.95 (s, 3H), 20.62 (s, 1H), 33.68 (s, 3H), 38.27 (s, 1H), 76.8 (br,  $v_{1/2}$  = 800 Hz, BH₄), 95.86 (s, 1H). Anal. calcd. for C₆4H₁2₆B₆MgN₄Nd₂O₆: C, 53.93; H, 8.91; N, 3.93. Found: 53.84; H, 8.82; N, 3.87. Crystals suitable for XRD were obtained from a concentrated solution in THF at -40 °C with a layer of pentane and revealed the molecular structure of

 $(PyA^2)Nd(THF)_2(BH_4)_2$  (3'Nd). The <sup>1</sup>H NMR analysis of 3'Nd (Fig. S9) was similar to that of 3Nd (Fig. S8, SI section<sup>†</sup>).

Attempted preparation of  $[(PyA^3)Y(BH_4)_3]^2[Mg(THF)_6]^{2+}$ : a colorless solution of  $Y(BH_4)_3(THF)_3$  (0.147 g, 0.42 mmol) and  $PyAH^3$  (0.210 g, 0.42 mmol) in toluene was treated with half an equiv. of BEM (BEM solution in hexane at 1.28 M) (0.16 mL, 0.21 mmol). Upon addition of BEM, the solution turned from orange to purple with the presence of a white precipitate. This solution was left under stirring for 30 minutes. Evaporation of the solvents afforded a purple foam to which toluene (15 mL) was added. Subsequent filtration and evaporation resulted in a purple powder (0.135 g). Several attempts of crystallization resulted only by the obtention of a small crop (ca. 30 mg) of brown crystals of  $(PyA^3)Mg(BH_4)$  according to XRD analysis.

Isolation of [(PyA(EA))Y(BH<sub>4</sub>)<sub>2</sub>][Li(THF)<sub>4</sub>]) (5<sub>Y</sub>) from the attempted preparation of (PyA<sup>3</sup>)Y(BH<sub>4</sub>)<sub>2</sub>: a colorless solution of Y(BH<sub>4</sub>)<sub>3</sub>(THF)<sub>3</sub> (0.246 g, 0.7 mmol) and PyAH<sup>3</sup> (0.350 g, 0.7 mmol) in THF was treated with 1 equiv. of "BuLi ("BuLi solution in hexane at 1.6 M) (0.44 mL, 0.7 mmol) at room temperature. Upon addition of "BuLi, the solution turned from colorless to dark red and was left stirred for 15 min. The THF was removed under *vacuum*, and the red product was washed with 20 mL of pentane. The complex was than dissolved in toluene, filtered and allow to stand at room temperature with diffusion of pentane to yield red crystals (150 mg) of [(PyA(EA))Y(BH<sub>4</sub>)<sub>2</sub>][Li(THF)<sub>4</sub>]. The <sup>1</sup>H NMR spectra in C<sub>6</sub>D<sub>6</sub> and THF-D<sub>8</sub> are displayed in Figs. S10 and S11, respectively, SI section†. The <sup>13</sup>C NMR spectrum is displayed in Fig. S12, SI section†. Anal. Calc. for C<sub>50</sub>H<sub>85</sub>B<sub>2</sub>LiN<sub>3</sub>O<sub>4</sub>Y: C, 66.02; H, 9.42; N, 4.62. Found: C, 63.84; H, 9.77; N, 4.22. Repeated analyses consistently gave carbon values that were slightly lower than expected for this product, even for crystalline samples.

**Preparation of (PyA³)Nd(BH**<sub>4</sub>)<sub>2</sub> (**4**<sub>Nd</sub>): a solution of Nd(BH<sub>4</sub>)<sub>3</sub>(THF)<sub>3</sub> (0.167 g, 0.4 mmol) and 1 equiv. **PyAH³** (0.200 g, 0.4 mmol) in toluene (10 mL) was treated with a 1.28 M solution of BEM in hexane (0.16 mL, 0.2 mmol, 0.5 equiv.). The solution turned from orange to purple with a white solid and was left to stir for 1 h at room temperature. After evaporation of the THF, the purple-red oil was extracted with 20 mL of toluene (red solution) and concentrated to half of the solution, then left at room temperature for crystallization. 0.077 g of red crystals (0.11 mmol, 29%) were obtained and the resulting solution was dried under *vacuum* to yield a red powder (0.072 g, 0.10 mmol, 27%). <sup>1</sup>H NMR (300 MHz, THF-D<sub>8</sub>, Fig. S12, SI section†): δ (ppm) = -13.58 (s, 6H), -8.21 (s, 1H), -7.31(s, 3H), -1.85 (s, 6H), 2.27 (s, 1H), 6.54 (s, 6H), 8.83 (br, 2H), 9.05 (br s, 1H ) 13.15 (s, 1H), 13.77 (s, 2H), 18.51 (s, 6H), 19.37 (s, 1H), 23.22 (s, 2H), 61.68 (br, BH<sub>4</sub>), 97.48 (br, 2H). Anal. Calc. for C<sub>38</sub>H<sub>62</sub>B<sub>2</sub>N<sub>3</sub>NdO (THF adduct): C, 61.45; H, 8.41; N, 5.66. Found: C, 61.17; H, 8.59; N, 5.44.

#### **Data availability**

The data supporting this article have been included as part of the SI.†

#### **Author contributions**

MB carried out the synthesis, NMR characterization and polymerization catalysis, and made a preliminary contribution to the writing. YC and MV designed the research, carried out complementary syntheses and characterizations and directed the experimental work, and wrote the article equally. FD solved the crystal structures with the exception of the KN.PyAH¹ complex, which was solved by JWZ. WJE took part in discussions especially on ligands syntheses and contributed to the writing and proof-reading. The manuscript was written through contributions of all authors. All authors have given approval to the final version of the manuscript.

#### **Conflicts of interest**

There are no conflicts to declare

#### Acknowledgements

We warmly thank the University of Lille for the financial support to MB and the CNRS for partially funding this work. The U. S. National Science Foundation is thanked for support under CHE-2154255 (WJE and JWZ). Aurélie Malfait and Dr Jonathan Potier are acknowledged for SEC analyses. Dr Eric Buisine is gratefully thanked for assistance with NMR spectroscopy, as well as Céline Delabre for elemental analyses.

† Supplementary information (SI) available: Crystal data refinement,  $^1H$  NMR spectra and SEC chromatograms. CCDC 2371034 ( $^1_{Y}$ ), 2371035 [KN(SiMe<sub>3</sub>)<sub>2</sub>.PyAH<sup>1</sup>], 2371036 ( $^1_{Z}$ ), 2371037 ( $^1_{Z}$ ), 2371038 (( $^1_{Z}$ )-Mg), 2371039 ( $^1_{Z}$ ), 2371040 ( $^1_{Z}$ ), 2371041 (( $^1_{Z}$ )-Mg), 2371042 ( $^1_{Z}$ ), 2371043 ( $^1_{Z}$ ), 2371044 ( $^1_{Z}$ ).

#### References

- (a) S.-F. Yuan, Y. Yan, G. A. Solan, Y. Ma and W.-H. Sun, Recent advancements in N-ligated group 4 molecular catalysts for the (co)polymerization of ethylene, *Coord. Chem. Rev.*, 2020, 411, 213254; (b) A. J. L. Pombeiro, Nitrogen ligands, *Dalton Trans.*, 2019, 48, 13904; (c) G. Chelucci, Metal-complexes of optically active amino-and imino-based pyridine ligands in asymmetric catalysis, *Coord. Chem. Rev.*, 2013, 257, 1887; (d) G. Ricci, A. Sommazzi, F. Masi, M. Ricci, A. Boglia and G. Leone, Well-defined transition metal complexes with phosphorus and nitrogen ligands for 1,3-dienes polymerization, *Coord. Chem. Rev.*, 2010, 254, 661; (e) M. Kruppa and B. König, Reversible Coordinative Bonds in Molecular Recognition, *Chem. Rev.*, 2006, 106, 3520; (f) G. Giambastiani and J. Campora, *Olefin Upgrading Catalysis by Nitrogen-based Metal Complexes, I and II*, Springer, London, 2011.
- (a) M. Westerhausen, T. Bollwein, N. Makropoulos, T. M. Rotter, T. Habereder, M. Suter and H. Nöth, The Metalation of (tert-Butyldimethylsilyl)(2-pyridylmethyl)amine with Dimethylzinc and Subsequent Zinc-Mediated Carbon-Carbon Coupling Reaction, Eur. J. Inorg. Chem., 2001, 851; (b) M. Westerhausen, T. Bollwein, N. Makropoulos, S. Schneiderbauer, M. Suter, H. Nöth, P. Mayer, H. Piotrowski, K. Polborn and A. Pfitzner, Zinc- and Tin-Mediated C-C Coupling Reactions of Metalated (2-Pyridylmethyl)(trialkylsilyl)amines Mechanistic, NMR Spectroscopic, and Structural Studies, Eur. J. Inorg. Chem., 2002, 389.
- For example: (a) Y.-C. Lin, K.-H. Yu, S.-L. Huang, Y.-H. Liu, Y. Wang, S.-T. Liu and J.-T. Chen, Alternating ethylene-norbornenecopolymerization catalyzed by cationic organopalladium complexes bearing hemilabile bidentate ligands of α-amino-pyridines, Dalton Trans., 2009, 41, 9058; (b) S. Zai, F. Liu, H. Gao, C. Li, G. Zhou, S. Cheng, L. Guo, L. Zhang, F. Zhu and Q. Wu, Longstanding living polymerization of ethylene: substituent effect on bridging carbon of 2-pyridinemethanamine nickelcatalysts, Chem. Commun., 2010, 46, 4321; (c) Y.-C. Lin, K.-H. Yu, Y.-F. Lin, G.-H. Lee, Y. Wang, S.-T. Liu and J.-T. Chen, Synthesis, structures of (aminopyridine) nickel complexes and their use for catalytic ethylene polymerization, Dalton Trans., 2012, 41, 6661; (d) K.-H. Yu, S.-L. Huang, Y.-H. Liu, Y. Wang, S.-T. Liu, Y.-C. Cheng, Y.-F. Lin and J.-T. Chen, Kinetics, Mechanism and Theoretical Studies of Norbornene-Ethylene Alternating Copolymerization Catalyzed by Organopalladium(II) Complexes Bearing Hemilabile α-Amino-pyridine, Molecules, 2017, 22, 1095; (e) D. M. Lovett, L. M. Thierer, E. E. P. Santos, R. L. Hardie, W. G. Dougherty, N. A. Piro, W. S. Kassel, B. M. Cromer, E. B. Coughlin and D. L. Zubris, Nickel (II) complexes bearing 2-ethylcarboxylate-6-iminopyridyl ligands: synthesis, structures and their catalytic behavior for ethylene oligomerization and polymerization, J. Organomet. Chem., 2018, 863, 44; (f) T. R. Boussie, G. M. Diamond, C. Goh, K. A. Hall, A. M. LaPointe, M. K. Leclerc, V. Murphy, J. A. W. Shoemaker, H. Turner, R. K. Rosen, J. C. Stevens, F. Alfano, V. Busico, R. Cipullo and G. Talarico, Nonconventional Catalysts for Isotactic Propene Polymerization in Solution Developed by Using High-Throughput-Screening Technologies, Angew. Chem., Int. Ed., 2006, 45, 3278; (g) D. J. Arriola, E. M. Carnahan, P. D. Hustad, R. L. Kuhlman and T. T. Wenzel, Catalytic Production of Olefin Block Copolymers via Chain Shuttling Polymerization, Science, 2006, 312, 714; (h) R. D. J. Froese, P. D. Hustad, R. L. Kuhlman and T. T. Wenzel, Mechanism of Activation of a Hafnium Pyridyl-Amide Olefin Polymerization Catalyst: Ligand Modification by Monomer, J. Am. Chem. Soc., 2007, 129, 7831; (i) C. Zuccaccia, A. Macchioni, V. Busico, R. Cipullo, G. Talarico, F. Alfano, H. W. Boone, K. A. Frazier, P. D. Hustad, J. C. Stevens, P. C. Vosejpka and K. A.

Abboud, Intra- and Intermolecular NMR Studies on the Activation of Arylcyclometallated Hafnium Pyridyl-Amido Olefin Polymerization Precatalysts, *J. Am. Chem. Soc.*, 2008, **130**, 10354; (*j*) C. Zuccaccia, V. Busico, R. Cipullo, G. Talarico, R. D. J. Froese, P. C. Vosejpka, P. D. Hustad and A. Macchioni, On the First Insertion of  $\alpha$ -Olefins in Hafnium Pyridyl-Amido Polymerization Catalysts, *Organometallics*, 2009, **28**, 5445; (*k*) G. J. Domski, E. B. Lobkovsky and G. W. Coates, Polymerization of  $\alpha$ -Olefins with Pyridylamidohafnium Catalysts: Living Behavior and Unexpected Isoselectivity from a *Cs*-Symmetric Catalyst Precursor, *Macromolecules*, 2007, **40**, 3510; (*I*) L. Annunziata, S. Pragliola, D. Pappalardo, C. Tedesco and C. Pellecchia, New (Anilidomethyl)pyridine Titanium(IV) and Zirconium(IV) Catalyst Precursors for the Highly Chemo- and Stereoselective *cis*-1,4-Polymerization of 1,3-Butadiene, *Macromolecules*, 2011, **44**, 1934.

- <sup>4</sup> O. H. Hashmi, F. Capet, M. Visseaux and Y. Champouret, Homoleptic and Heteroleptic Substituted Amidomethylpyridine Iron Complexes: Synthesis, Structure and Polymerization of rac-Lactide, *Eur. J. Inorg. Chem.*, 2022, **15**, e202200073
- (a) S. Nayab, H. Lee and J. H. Jeong, Zinc complexes bearing N,N'-bidentate entiopure ligands: Synthesis, structure and catalytic activity toward ring opening polymerisation of rac-lactide, *Polyhedron*, 2012, 43, 55; (b) H. Ahn, M. K. Chun, E. Kim, J. H. Jeong, S. Nayab and H. Lee, Copper(II) complexes containing N,N'-bidentate N-substituted N-(pyridin-2-ylmethyl)amine: Synthesis, structure and application towards polymerization of rac-lactide, *Polyhedron*, 2017, 127, 51; (c) J. Cho, M. K. Chun, S. Nayab and J. H. Jeong, Synthesis and structures of copper(II) complexes containing N,N-bidentate N-substituted phenylethanamine derivatives as pre-catalysts for heterotactic-enriched polylactide, *Polyhedron*, 2019, 163, 54.
- (a) F. T. Edelmann, D. M. M. Freckmann and H. Schumann, Synthesis and Structural Chemistry of Non-Cyclopentadienyl Organolanthanide Complexes, Chem. Rev., 2002, 102, 1851; (b) W. E. Piers and D. J. H. Emslie, Non-cyclopentadienyl ancillaries in organogroup 3 metal chemistry: a fine balance in ligand design, Coord. Chem. Rev., 2002, 233-234, 131; (c) M. Zimmermann and R. Anwander, Homoleptic Rare-Earth Metal Complexes Containing Ln–C σ-Bonds, Chem. Rev., 2010, 110, 6194; (d) F. Ortu, Rare Earth Starting Materials and Methodologies for Synthetic Chemistry, Chem. Rev., 2022, 122, 6040; (e) M. Beauvois, Y. Champouret, F. Bonnet and M. Visseaux (2022) Alkenes and Allyl Complexes of the Group 3 Metals and Lanthanides. In: Parkin, G., Meyer, K., O'Hare, D. (eds.) Comprehensive Organometallic Chemistry IV. vol. 3, pp. 382-448. Kidlington, UK: Elsevier; (f) M. Visseaux and F. Bonnet, Borohydride complexes of rare earths, and their applications in various organic transformations, Coord. Chem. Rev. 2011, 255, 374; (g) O. T. Summerscales and J. C. Gordon, Complexes containing multiple bonding interactions between lanthanoid elements and main-group fragments, RSC Adv., 2013, 3, 6682; (h) P. L. Arnold and I. J. Casely, F-Block N-Heterocyclic Carbene Complexes, Chem. Rev. 2009, 109, 3599; (i) N. Marques, A. Sella and J. Takats, Chemistry of the Lanthanides Using Pyrazolylborate Ligands, Chem. Rev. 2002, 102, 2137; (j) M. N. Bochkarev, Synthesis, Arrangement, and Reactivity of Arene-Lanthanide Compounds, Chem. Rev. 2002, 102, 2089; (k) F. Nief, Heterocyclopentadienyl Complexes of Group-3 Metals, Eur. J. Inorg. Chem. 2001, 891; (I) B. D. Ward and L. H. Gade, Rare earth metaloxazoline complexes in asymmetric catalysis, Chem. Commun., 2012, 48, 10587; (m) S. Kobayashi, M. Sugiura, H. Kitagawa and W. W.-L. Lam, Rare-Earth Metal Triflates in Organic Synthesis, Chem. Rev. 2002, 102, 2227; (n) C. Schädle, C. Meermann, K. W. Törnroos and R. Anwander, Rare-Earth Metal Phenyl(trimethylsilyl)amide Complexes, Eur. J. Inorg. Chem. 2010, 2841.
- (a) A. A. Kissel and A. A. Trifonov, N-Containing Ligands as Universal Coordination Environments for Rare-Earth Alkyl and Bis(alkyl) Complexes, INEOS OPEN, 2018, 1, 1; (b) A. A. Trifonov, Guanidinate and amidopyridinate rare-earth complexes: Towards highly reactive alkyl and hydrido species, Coord. Chem. Rev., 2010, 254, 1327.
- T. M. Cameron, J. C. Gordon, R. Michalczyk and B. L. Scott, Unusual alkyl group activation and cationic complex formation from a novel lutetium dialkyl complex supported by a tridentate monoanionic ligand, *Chem. Commun.*, 2003, 2282.
- (a) F. Estler, G. Eickerling, E. Herdtweck and R. Anwander, Organo-Rare-Earth Complexes Supported by Chelating Diamide Ligands, *Organometallics*, 2003, 22, 1212; (b) M. Zimmermann, F. Estler, E. Herdtweck, K. W. Törnroos and R. Anwander, Distinct C- H Bond Activation Pathways in Diamido-Pyridine-Supported Rare-Earth Metal Hydrocarbyl Complexes, *Organometallics*, 2007, 26, 6029; (c) M. Zimmermann, K. W. Törnroos and R. Anwander, Alkyl Migration and an Unusual Tetramethylaluminate Coordination Mode: Unexpected Reactivity of Organolanthanide Imino-Amido-Pyridine Complexes, *Angew. Chem., Int. Ed.*, 2007, 46, 3126; (d) M. Zimmermann, K. W. Törnroos, R. M. Waymouth and R. Anwander, Structure-Reactivity Relationships of Amido-Pyridine-Supported Rare-Earth-Metal Alkyl Complexes, *Organometallics*, 2008, 27, 4310.
- (a) D. M. Lyubov, G. K. Fukin, A. V. Cherkasov, A. S. Shavyrin, A. A. Trifonov, L. Luconi, C. Bianchini, A. Meli and G. Giambastiani, Selective σ-Bond Metathesis in Alkyl–Aryl and Alkyl–Benzyl Yttrium Complexes. New Aryl–and Benzyl–Hydrido Yttrium Derivatives Supported by Amidopyridinate Ligands, *Organometallics*, 2009, 28,

- 1227; (b) L. Luconi, D. M. Lyubov, C. Bianchini, A. Rossin, C. Faggi, G. K. Fukin, A. V. Cherkasov, A. S. Shavyrin, A. A. Trifonov and G. Giambastiani, Yttrium-Amidopyridinate Complexes: Synthesis and Characterization of Yttrium-Alkyl and Yttrium-Hydrido Derivatives, *Eur. J. Inorg. Chem.*, 2010, 608; (c) A. A. Karpov, A. V. Cherkasov, G. K. Fukin, A. S. Shavyrin, L. Luconi, G. Giambastiani and A. A. Trifonov, Yttrium Complexes Featuring Different Y–C Bonds. Comparative Reactivity Studies: Toward Terminal Imido Complexes, *Organometallics*, 2013, **32**, 2379.
- (a) L. Luconi, D. M. Lyubov, A. Rossin, T. A. Glukhova, A. V. Cherkasov, G. Tuci, G. K. Fukin, A. A. Trifonov and G. Giambastiani, Organolanthanide Complexes Supported by Thiazole-Containing Amidopyridinate Ligands: Synthesis, Characterization, and Catalytic Activity in Isoprene Polymerization, Organometallics, 2014, 33, 7125; (b) D. M. Lyubov, L. Luconi, A. Rossin, G. Tuci, A. V. Cherkasov, G. K. Fukin, G. Giambastiani and A. A. Trifonov, Metal-to-Ligand Alkyl Migration Inducing Carbon–Sulfur Bond Cleavage in Dialkyl Yttrium Complexes Supported by Thiazole-Containing Amidopyridinate Ligands: Synthesis, Characterization, and Catalytic Activity in the Intramolecular Hydroamination Reaction, Chem. Eur. J., 2014, 20, 3487.
- (a) X. Zhang, S. Zhou, X. Fang, L. Zhang, G. Tao, Y. Wei, X. Zhu, P. Cui and S. Wang, Syntheses of Dianionic α-Iminopyridine Rare-Earth Metal Complexes and Their Catalytic Acitivities toward Dehydrogenative Coupling of Amines with Hydrosilanes, *Inorg. Chem.*, 2020, 59, 9683; (b) X. Zhang, S. Zhou, D. Wang, L. Zhang, Y. Wei, X. Zhu, P. Cui, G. Luo and S. Wang, Syntheses of Rare-Earth Metal Alkyl Complexes Bearing a Dianionic α-Iminopyridyl Ligand and Their Catalytic Activities toward Polymerization of 2-Vinylpyridine, *Organometallics*, 2021, 40, 3462.
- <sup>13</sup> Z. Jian and D. Cui, Rare-earth metal bis(alkyl)s that bear a 2-pyridinemethanamineligand: Dual catalysis of the polymerizations of both isoprene and ethylene, *Dalton Trans.*, 2012, **41**, 2367.
- D. Liu, Y. Luo, W. Gao and D. Cui, Stereoselective Polymerization of Styrene with Cationic Scandium Precursors Bearing Quinolyl Aniline Ligands, *Organometallics*, 2010, **29**, 1916.
- D. Liu and D. Cui, Highly *trans-*1,4 selective (co-)polymerization of butadiene and isoprene with quinolyl anilido rare earth metal bis(alkyl) precursors, *Dalton Trans.*, 2011, **40**, 7755.
- D. Liu, M. Wang, Y. Chai, X. Wan and D. Cui, Self-Activated Coordination Polymerization of Alkoxystyrenes by a Yttrium Precursor: Stereocontrol and Mechanism, *ACS Catal.*, 2019, **9**, 2618.
- Y. Huo, X. Hu, J. Wang, H. Hu and X. Shi, Amido-trihydroquinoline ligated rare-earth metal complexes for polymerization of isoprene, *New J. Chem.*, 2022, **46**, 8277.
- (a) K. Nienkemper, G. Kehr, S. Kehr, R. Fröhlich and G. Erker, (Amidomethyl)pyridine zirconium and hafnium complexes: Synthesis and structural characterization, *J. Organomet. Chem.*, 2008, 693, 1572; (b) B.-Y. Tay, C. Wang, S.-C. Chia, L. P. Stubbs, P.-K. Wong and M. van Meurs, Synthesis of Bis(amino)pyridines by the Stepwise Alkylation of Bis(imino)pyridines: An Unexpected and Selective Alkylation of the Aminoiminopyridine by AlMe<sub>3</sub>, *Organometallics*, 2011, 30, 6028; (c) G. J. P. Britovsek, M. Bruce, V. C. Gibson, B. Kimberley, P. J. Maddox, S. Mastroianni, S. J. McTavish, C. Redshaw, G. A. Solan, S. Strömberg, A. J. P. White and D. J. Williams, Iron and Cobalt Ethylene Polymerization Catalysts Bearing 2,6-Bis(Imino)Pyridyl Ligands: Synthesis, Structures, and Polymerization Studies, *J. Am. Chem. Soc.*, 1999, 121, 8728.
- <sup>19</sup> A. Bondi, van der Waals Volumes and Radii, *J. Phys. Chem.*, 1964, **68**, 441.
- G. G. Skvortsov, M. V. Yakovenko, G. K. Fukin, E. V. Baranov, Yu. A. Kurskii and A. A. Trifonov, Synthesis, molecular structure, and catalytic activity of borohydride complexes [(Me<sub>3</sub>Si)<sub>2</sub>NC(NPri)<sub>2</sub>]<sub>2</sub>Nd(BH<sub>4</sub>)<sub>2</sub>Li(thf)<sub>2</sub> and [(Me<sub>3</sub>Si)<sub>2</sub>NC(NPri)<sub>2</sub>]<sub>2</sub>Sm(BH<sub>4</sub>)<sub>2</sub>Li(thf)<sub>2</sub>, Russ. Chem. Bull. Int. Ed., 2007, **56**, 456.
- (a) D. Barbier-Baudry, F. Bouyer, A. S. M. Bruno and M. Visseaux, Lanthanide borohydrido complexes for MMA polymerization: syndio- vs iso- stereocontrol, Appl. Organomet. Chem., 2006, 20, 24; (b) M. Visseaux, T. Chenal, P. Roussel and A. Mortreux, Synthesis and X-ray structure of a borohydrido metallocene of neodymium and its use as pre-catalyst in Nd/Mg dual-component ethylene and isoprene polymerisations, J. Organomet. Chem., 2006, 691, 86; (c) F. Bonnet, M. Visseaux, A. Hafid, D. Baudry-Barbier, M. M. Kubicki and E. Vigier, Structural diversity in the borohydrido lanthanides series: First isolation and X-ray crystal structure of ionic [Sm(BH<sub>4</sub>)<sub>2</sub>(THF)<sub>5</sub>]+[Cp\*'Sm(BH<sub>4</sub>)<sub>3</sub>]-, Inorg. Chem. Comm., 2007, 10, 690; (d) F. Bonnet, C. Da Costa Violante, P. Roussel, A. Mortreux and M. Visseaux, Unprecedented dual behaviour of a half-sandwich scandium-based initiator for both highly selective isoprene and styrene polymerisation, Chem. Commun., 2009, 23, 3380; (e) Jaroschik, F. Bonnet, X.F. Le Goff, L. Ricard, F. Nief and M. Visseaux, Synthesis of samarium(II) borohydrides and their behaviour as initiators in styrene and ε-caprolactone polymerisation, Dalton Trans., 2010, 39, 6761.
- <sup>22</sup> K. F. Tesh, T. P. Hanusa and J. C. Huffman, Ion pairing in [bis (trimethylsilyl) amido] potassium: The x-ray crystal structure of unsolvated [KN(SiMe<sub>3</sub>)<sub>2</sub>]<sub>2</sub>, *Inorg. Chem.*, 1990, **29**, 1584.
- (a) M. Visseaux, M. Terrier, A. Mortreux and P. Roussel, One-pot synthesis of an ionic half-sandwich complex of neodymium. Application to isoprene polymerisation catalysis, *C. R. Chimie*, 2007, **10**, 1195; (b) M. Visseaux,

- P. Zinck, M. Terrier, A. Mortreux and P. Roussel, New ionic half-metallocenes of early lanthanides, *J. All. Comp.*, 2008, **451**, 352; (*c*) P. Zinck, A. Valente, M. Terrier, A. Mortreux and M. Visseaux, Half-lanthanidocenes catalysts via the "borohydride/alkyl" route: A simple approach of ligand screening for the controlled polymerization of styrene, *C. R. Chimie*, 2008, **11**, 595; (d) M. Visseaux, M. Terrier, A. Mortreux and P. Roussel, Facile Synthesis of Lanthanidocenes by the "Borohydride/Alkyl Route" and Their Application in Isoprene Polymerization, *Eur. J. Inorg. Chem.*, 2010, 2867.
- Ligands redistribution in organolanthanide chemistry has been well documented: (a) G. V. Khoroshen'kov, A. A. Fagin, M. N. Bochkarev, S. Dechert and H. Schumann, Reactions of neodymium(ii), dysprosium(ii), and thulium(ii) diiodides with cyclopentadiene. Molecular structures of complexes CpTml<sub>2</sub>(THF)<sub>3</sub> and [Ndl<sub>2</sub>(THF)<sub>5</sub>]<sup>+</sup>[Ndl<sub>4</sub>(THF)<sub>2</sub>]<sup>-</sup>, Russ. Chem. Bull., 2003, 52, 1715; (b) P. L. Arnold and S. T. Liddle, Deprotonation of N-Heterocyclic Carbenes to Afford Heterobimetallic Organolanthanide Complexes, Organometallics, 2006, 25, 1485; (c) C. Pi, Z. Zhu, L. Weng, Z. Chen and X. Zhou, Synthesis and structural characterization of lanthanide complexes with the di- or tri-anionic diguanidinate ligand: new insight into the flexibility and distinct reactivity of the linked diguanidinate ligand, Chem. Commun., 2007, 21, 2190.
- (a) S. Fadlallah, M. Terrier, C. Jones, P. Roussel, F. Bonnet and M. Visseaux, Mixed Allyl–Borohydride Lanthanide Complexes: Synthesis of Ln(BH<sub>4</sub>)<sub>2</sub>(C<sub>3</sub>H<sub>5</sub>)(THF)<sub>3</sub> (Ln = Nd, Sm), Characterization, and Reactivity toward Polymerization, *Organometallics*, 2016, 35, 456; (b) S. Fadlallah, J. Jothieswaran, F. Capet, F. Bonnet and M. Visseaux, Mixed Allyl Rare-Earth Borohydride Complexes: Synthesis, Structure, and Application in (Co-)Polymerization Catalysis of Cyclic Esters, *Chem. Eur. J.* 2017, 23, 15644 (c) S. Fadlallah, J. Jothieswaran, I. Del Rosal, L. Maron, F. Bonnet and M. Visseaux, Rationalizing the Reactivity of Mixed Allyl Rare-Earth Borohydride Complexes with DFT Studies, *Catalysts*, 2020, 10, 820.
- <sup>26</sup> L. F. Sánchez-Barba, D. L. Hughes, S. M. Humphrey and M. Bochmann, Ligand Transfer Reactions of Mixed-Metal Lanthanide/Magnesium Allyl Complexes with β-Diketimines: Synthesis, Structures, and Ring-Opening Polymerization Catalysis, *Organometallics*, 2006, **25**, 1012.
- <sup>27</sup> B. M. Lindley, P. T. Wolczanski, T. R. Cundari and E. B. Lobkovsky, First-Row Transition Metal and Lithium Pyridine-ene-amide Complexes Exhibiting N- and C-Isomers and Ligand-Based Activation of Benzylic C–H Bonds, *Organometallics*, 2015, **34**, 4656–4668.
- A. W. Addison, T. N. Rao, J. Reedijk, J. van Rijn and G. C. Verschoor, Synthesis, structure, and spectroscopic properties of copper(II) compounds containing nitrogen—sulphur donor ligands; the crystal and molecular structure of aqua[1,7-bis(N-methylbenzimidazol-2'-yl)-2,6-dithiaheptane]copper(II) perchlorate, *J. Chem. Soc., Dalton Trans.*, 1984, **7**, 1349. The calculation of this  $\tau$  parameter in a five substituents system such as this one allows us to determinate the constraint on the metal and the percentage of distortion from a square pyramidal to a trigonal bipyramidal geometry. The value of  $\tau$  oscillates between 0 and 1 where 0 correspond to a perfect square pyramidal geometry and 1 to a trigonal bipyramidal geometry. This geometric parameter was determined by the equation:  $\tau = (\beta \alpha)/60$  where  $\beta$  is the largest angle of the base (here N1-Y-B1 = 155.9°) and  $\alpha$  is the second largest angle (here N2-Y-B2: 128.2°).
- <sup>29</sup> (a) M. Ephritikhine, Chem. Rev. 97 (1997) 2193; (b) Makhaev, V. D., Structural and dynamic properties of tetrahydroborate complexes, *Russ. Chem. Rev.*, 2000, **69**, 727.
- S. M. Cendrowski-Guillaume, M. Nierlich, M. Lance and M. Ephritikhine, First Chemical Transformations of Lanthanide Borohydride Compounds: Synthesis and Crystal Structures of [(η-C<sub>8</sub>H<sub>8</sub>)Nd(BH<sub>4</sub>)(THF)]<sub>2</sub> and [(η-C<sub>8</sub>H<sub>8</sub>)Nd(THF)<sub>4</sub>][BPh<sub>4</sub>], Organometallics, 1998, 17, 786.
- R. D. Shannon, Revised effective ionic radii and systematic studies of interatomic distances in halides and chalcogenides, *Acta Cryst.*, 1976, **A32**, 751.
- <sup>32</sup> F. H. Allen, O. Kennard, D. G. Watson, L. Brammer, A. G. Orpen and R. J. Taylor, Tables of Bond Lengths determined by X-Ray and Neutron Diffraction. Part 1. Bond Lengths in Organic Compounds, *J. Chem. Soc., Perkin Trans.* 2, 1987, S1—S19.
- S. S. Galley, S. A. Pattenaude, R. F. Higgins, C. J. Tatebe, D. A. Stanley, P. E. Fanwick, M. Zeller, E. J. Schelter and S. C. Bart, A reduction series of neodymium supported by pyridine(diimine) ligands, *Dalton Trans.*, 2019, 48, 8021.
- D. M. Lyubov, A. O. Tolpygin and A. A. Trifonov, Rare-earth metal complexes as catalysts for ring-opening polymerization of cyclic esters, *Coord. Chem. Rev.*, 2019, **392**, 83.
- (a) O. Dechy-Cabaret, B. Martin-Vaca and D. Bourissou, Controlled Ring-Opening Polymerization of Lactide and Glycolide, *Chem. Rev.*, 2004, **104**, 6147; (b) E. Stirling, Y. Champouret and M. Visseaux, Catalytic metalbased systems for controlled statistical copolymerisation of lactide with a lactone, *Polym. Chem.*, 2018, **9**, 2517.

- I. Palard, M. Schappacher, B. Belloncle, A. Soum and S. M. Guillaume, Unprecedented Polymerization of Trimethylene Carbonate Initiated by a Samarium Borohydride Complex: Mechanistic Insights and Copolymerization with ε-Caprolactone, Chem. Eur. J., 2007, 13, 1511.
- 37 (a) S. M. Guillaume, M. Schappacher and A. Soum, Polymerization of ε-Caprolactone Initiated by Nd(BH<sub>4</sub>)<sub>3</sub>(THF)<sub>3</sub>: Synthesis of Hydroxytelechelic Poly(ε-caprolactone), *Macromolecules*, 2003, **36**, 54; (b) I. Palard, A. Soum and S. M. Guillaume, Rare Earth Metal Tris(borohydride) Complexes as Initiators for ε-Caprolactone Polymerization: General Features and IR Investigations of the Process, *Macromolecules*, 2005, **38**, 6888.
- Selected references: (a) X. Shen, M. Xue, R. Jiao, Y. Ma, Y. Zhang and Q. Shen, Bis(β-diketiminate) Rare-Earth-Metal Borohydrides: Syntheses, Structures, and Catalysis for the Polymerizations of l-Lactide, ε-Caprolactone, and Methyl Methacrylate, Organometallics, 2012, 31, 6222; (b) M. V. Yakovenko, A. A. Trifonov, E. Kirillov, T. Roisnel and J.-F. Carpentier, Lanthanide borohydrides supported by an ansa-bis(amidinate) ligand with a rigid naphthalene linker: Synthesis, structure and catalytic activity in ring-opening polymerization of lactide, Inorg. Chim. Acta, 2012, 383, 137; (c) M. Schmid, P. Oña-Burgos, S. M. Guillaume and P. W. Roesky, (Iminophosphoranyl)(thiophosphoranyl)methane rare-earth borohydride complexes: synthesis, structures and polymerization catalysis, Dalton Trans., 2015, 44, 12338; (d) T. P. Seifert, T. S. Brunner, T. S. Fischer, C. Barner-Kowollik and P. W. Roesky, Chiral Mono(borohydride) Complexes of Scandium and Lutetium and Their Catalytic Activity in Ring-Opening Polymerization of DL-Lactide, Organometallics, 2018, 37, 4481; (e) D. A. Bardonov, P. D. Komarov, G. I. Sadrtdinova, V. K. Besprozvannyh, K. A. Lyssenko, A. O. Gudovannyy, I. E. Nifant'ev, M. E. Minyaev and D. M. Roitershtein, Cyclopentadienyl lanthanide borohydrides derived from the unsubstituted cyclopentadienyl ligand. Unprecedented structural diversity and ε-caprolactone polymerization, Inorg. Chim. Acta, 2022, 529, 120638; (f) M. A. Sinenkov, G. K. Fukin, A. V. Cherkasov, N. Ajellal, T. Roisnel, F. M. Kerton, J.-F. Carpentier and A. A. Trifonov, Neodymium borohydride complexes supported by diamino-bis(phenoxide) ligands: diversity of synthetic and structural chemistry, and catalytic activity in ring-opening polymerization of cyclic esters, New J. Chem., 2011, 35, 204; (g) G. G. Skvortsov, A. S. Shavyrin, T. A. Kovylina, A. V. Cherkasov and A. A. Trifonov, Rare-Earth Amido and Borohydrido Complexes Supported by Tetradentate Amidinate Ligands: Synthesis, Structure, and Catalytic Activity in Polymerization of Cyclic Esters, Eur. J. Inorg. Chem., 2019, 5008.
- J. Kratsch, M. Kuzdrowska, M. Schmid, N. Kazeminejad, C. Kaub, P. Oña-Burgos, S. M. Guillaume and P. W. Roesky, Chiral Rare Earth Borohydride Complexes Supported by Amidinate Ligands: Synthesis, Structure, and Catalytic Activity in the Ring-Opening Polymerization of rac-Lactide, *Organometallics*, 2013, **32**, 1230.
- G. R. Fulmer, A. J. M. Miller, N. H. Sherden, H. E. Gottlieb, A. Nudelman, B. M. Stoltz, J. E. Bercaw and K. I. Goldberg, NMR Chemical Shifts of Trace Impurities: Common Laboratory Solvents, Organics, and Gases in Deuterated Solvents Relevant to the Organometallic Chemist, Organometallics, 2010, 29, 2176.
- <sup>41</sup> A. Duda, A. Kowalski and S. Penczek, Polymerization of *L,L*-Lactide Initiated by Aluminum Isopropoxide Trimer or Tetramer, *Macromolecules*, 1998, **31**, 2114..
- M. Save, M. Schappacher and A. Soum, Controlled Ring-Opening Polymerization of Lactones and Lactides Initiated by Lanthanum Isopropoxide, 1. General Aspects and Kinetics, *Macromol. Chem. Phys.*, 2002, 203, 889.
- <sup>43</sup> G. M. Sheldrick, SHELXT Integrated space-group and crystal-structure determination, *Acta Cryst. Sect. A*, 2015, **71**, 3.
- <sup>44</sup> G. M. Sheldrick, Crystal structure refinement with SHELXL, Acta Cryst. Sect. C, 2015, **71**, 3.
- <sup>45</sup> APEX2 Version 2014.11-0, Bruker AXS, Inc.; Madison, WI 2014.
- 46 SAINT Version 8.34a, Bruker AXS, Inc.; Madison, WI 2013
- Sheldrick, G. M. SADABS, Version 2014/5, Bruker AXS, Inc.; Madison, WI 2014.
- O. V. Dolomanov, L. J. Bourhis, R. J. Gildea, J. A. K. Howard and H. Puschmann, OLEX2: A complete structure solution, refinement and analysis program, *J. Appl. Cryst.*, 2009, **42**, 339.
- <sup>49</sup> C. F. Macrae, I. Sovago, S. J. Cottrell, P. T. A. Galek, P. McCabe, E. Pidcock, M. Platings, G. P. Shields, J. S. Stevens, M. Towler and P. A. Wood, Mercury 4.0: from visualization to analysis, design and prediction, *J. Appl. Cryst.*, 2020, **53**, 226.

## Synthesis and Characterization of Borohydride Rare-Earth Complexes Supported by 2-PyridinemethanAmido Ligands and their Application towards Ring-Opening Polymerization of Cyclic Esters

Maxime Beauvois,<sup>a</sup> Frédéric Capet,<sup>a</sup> Joseph W. Ziller,<sup>b</sup> William J. Evans,<sup>b</sup> Yohan Champouret,\*,<sup>a</sup> Marc Visseaux\*,<sup>a</sup>

#### **Data availability**

The data supporting this article have been included as part of the ESI.†

† Supplementary information (SI) available: Crystal data refinement,  $^1H$  NMR spectra and SEC chromatograms. CCDC 2371034 ( $^1_{Y}$ ), 2371035 [KN(SiMe<sub>3</sub>)<sub>2</sub>.PyAH<sup>1</sup>], 2371036 ( $^1_{Z}$ ), 2371037 ( $^1_{Z}$ ), 2371038 (( $^1_{Z}$ )-Mg), 2371039 ( $^1_{Z}$ ), 2371040 ( $^1_{Z}$ ), 2371041 (( $^1_{Z}$ )-Mg), 2371042 ( $^1_{Z}$ ), 2371043 ( $^1_{Z}$ ), 2371044 ( $^1_{Z}$ ).

<sup>&</sup>lt;sup>a</sup> Univ. Lille, CNRS, Centrale Lille, Univ. Artois, UMR 8181, UCCS, Unité de Catalyse et Chimie du Solide, F-59000, Lille, France. E-mail : Yohan.champouret@univ-lille.fr, Marc.visseaux@univ-lille.fr.

<sup>&</sup>lt;sup>b</sup> Department of Chemistry, University of California, Irvine, California 92697-2025, United States